Summer 2011

Age-Related Hamster Mitochondrial Changes and Oocyte Changes Following Autologous Platelet Mitochondrial Microinjection

Fang Li
Old Dominion University

AGE-RELATED HAMSTER MITOCHONDRIAL CHANGES AND OOCYTE CHANGES FOLLOWING AUTOLOGOUS PLATELET MITOCHONDRIAL MICROINJECTION

by

Fang Li
M.D. July 2000, Dalian Medical University, China
M.S. June 2003, China Medical University, China
M.S. December 2008, Old Dominion University

A Dissertation Submitted to the Faculty of
Old Dominion University in Partial Fulfillment of the
Requirements for the Degree of

DOCTOR OF PHILOSOPHY

BIOMEDICAL SCIENCES

OLD DOMINION UNIVERSITY
August 2011

Approved by:

R. James Swanson (Director)

Frank J. Castora (Member)

Christopher J. Osgood (Member)

David T. Gauthier (Member)

ABSTRACT

AGE-RELATED HAMSTER MITOCHONDRIAL CHANGES AND OOCYTE CHANGES FOLLOWING AUTOLOGOUS PLATELET MITOCHONDRIAL MICROINJECTION

Fang Li
Old Dominion University, 2011
Director: Dr. R. James Swanson

This study's objective was to verify age-related mitochondrial changes in oocytes from old hamsters compared with those from young hamsters. We used autologous platelet mitochondrial microinjection to improve the mitochondrial quality and quantity of aged oocytes to improve their pregnancy potential. Metaphase II oocytes were collected from super-ovulated female hamsters and prepared for biochemical and morphological analysis. Adenosine triphosphate (ATP) levels, mitochondrial DNA (mtDNA) number, reactive oxygen species (ROS) level and mitochondrial membrane potential (MMP) were determined in individual oocytes from young and old hamsters. Transmission electron microscopy (TEM) allowed evaluation of oocyte ultra-structure. In oocytes from old hamsters, ATP levels and mtDNA number were reduced an average of 35.4% and 51.8% respectively compared to young oocytes. Lower MMP and higher ROS levels were observed in oocytes from old hamsters compared with those from young hamsters. TEM analysis supported low mitochondrial quantity and increased mitochondrial electron density in old oocytes, along with collapsed cytoplasmic lamellae. When comparing platelet mitochondria between young and old hamsters, no significant difference was found in ATP level per mitochondrion or ultrastructure. After autologous platelet mitochondrial microinjection, ATP production increased significantly in the microinjected group, however mtDNA number and embryo development to blastocyst stage were not improved. MitoTracker Green FM (MGF) was used to help quantify mitochondria, but the results conflicted with mtDNA and TEM data, which suggests that MGF, as a MMP dependent reagent, is not an ideal method to reflect mitochondrial number. Our data suggest that (1) age-related morphological and functional mitochondrial changes occur in oocytes from old hamsters compared with young hamsters; (2) platelets can be used as a source for mitochondrial transfer; and (3) autologous platelet

mitochondrial microinjection improves mitochondrial ATP production in old oocytes. The fact that no change in blastocyst development after microinjection was observed does not rule out that there might not be improvement of post-implantation embryo development. Therefore, further study will focus on effect of autologous platelet mitochondrial microinjection on post-implantation embryo development.

This thesis is dedicated to my parents- ChangLin Li and Can Zhang; my husband-Yu Liu and my son-Brian Liu; my advisor- R. James Swanson, for their unselfish sacrifice, dedication and support throughout the completion of my PHD degree.

ACKNOWLEDGMENTS

I would like to thank Dr. R. James Swanson, who supported me as my advisor and guided my research project throughout my whole PHD program. Also thanks to my committee members, Dr. Frank J. Castora, Dr. Christopher J. Osgood and Dr. David T. Gauthier. Many thanks to Dr. Earl Godfrey for help on using transmission electron microscope and confocal microscope, Dr. Anna Jeng for help on fluorescence microscope. I wish to thank Kelly B. Wyatt for help on collecting oocytes, thank Dr. Wentia E. Ford for help on microinjection, and thank Dr. Fatma S. Duran for help on primer design and real-time PCR.

TABLE OF CONTENTS

LIST OF TABLES

LIST OF FIGURES

CHAPTER I

INTRODUCTION

BACKGROUND

Mammalian oocytes

Oocytes are mature female germ cells, derived from primordial germ cells (PGCs) which are descendants of the epiblast Mouse primordial germ cells are localized at the base of the allantois [1, 2] In humans, meiosis I of ootidogenesis of PGCs begins in the fetal ovary between 11 and 12 weeks of age PGCs undergo many cycles of mitotic division before entering the first stage of meiosis I, ultimately leading to the production of millions of oogonia [3] Oogonia enter the first meiotic division and arrest in prophase I as primary oocytes in the late fetal period, where they are surrounded by squamous precursors of follicular cells [4] A primary oocyte and its relatively undifferentiated granulosa cells enclosed by a basement membrane are recognized as a primordial follicle In both the rat and mouse, the formation of primordial follicles is completed by birth [5, 6], while in the hamster, germ cell mitosis continues for a few days after birth Therefore, germ cells, primordial oocytes and somatic cells are all found in the ovaries of a newborn hamster [7] In humans the primary oocytes halt in the diplotene stage of prophase I until puberty, and then a few continue to develop in each menstrual cycle The oocyte remains in the immature state because of many factors, such as oocyte maturation inhibitor secreted by granulosa cells At the start of the human menstrual cycle, some primary follicles begin to develop with increased follicle stimulating hormone (FSH) and only one (rarely two) healthy secondary follicle remain(s) growing by day 9 of the cycle. Other developed primary follicles undergo cellular atresia On day 14 of the cycle, a serum luteinizing hormone (LH) surge occurs As LH levels increase during the late preovulatory period, a number of events occur (1) the secondary follicle develops into a tertiary follicle which (2) becomes a mature follicle and ruptures (3) forming a corpus luteum from the empty follicle.

The LH surge is triggered by the positive feedback of estradiol 17-β. The primary oocyte completes the first meiotic division leading to the formation of a polar body and a secondary

---

The journal model is *Biology of Reproduction*

oocyte arrested at the metaphase II stage. [8, 9] (Fig. 1).

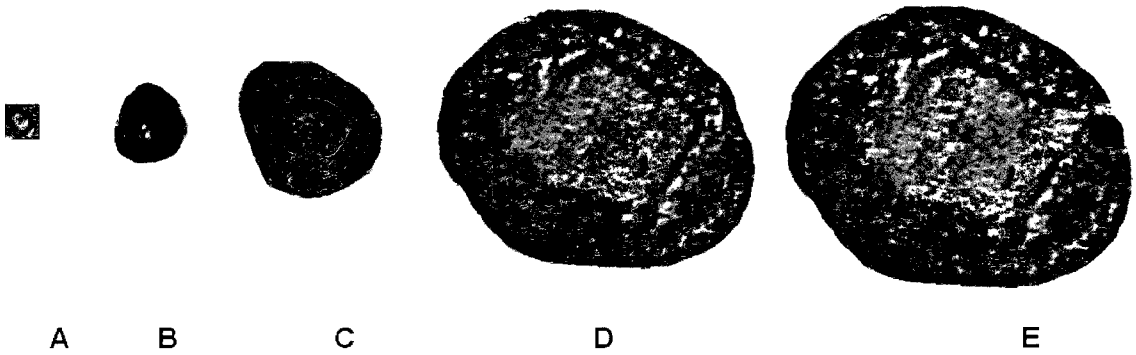

FIG. 1. Development of oocyte. Small **A)** primordial follicle develops into a **B)** primary follicle, then a **C)** secondary follicle and finally **D)** a fluid filled tertiary follicle (mature). This follicle may **E)** ovulate and become a corpus luteum

The quantity and quality of human follicles and their associated ova are major factors contributing to an age-related decline in fertility. Since the whole follicle pool is already laid down in the ovaries by the fifth intrauterine month in humans and a few days after birth in hamsters, damage can accumulate in follicles and ova as they age over years for humans or over months for hamster. At about 5 months in utero, the total number of follicles is established for the human reproductive lifespan, and their associated ova are aging from that fifth month on until the final ovulation at menopause. Follicles degenerate by a process called atresia either before or after initiating follicular growth [10]. Follicular depletion occurs faster than ovulation and only about 500 of 5 million oocytes will actually ovulate [11]. Accelerated atresia of the oocytes begins at an average age of 37.5 years (yrs) in humans, and starts at an earlier age in 10% of women [10]. Antral follicle count and basal serum levels of FSH are markers for ovarian reserve in normal women without polycystic ovaries, and a significant reduction in ovarian reserve occurs after the age of 35 yrs [12]. Obvious decline in fecundity has been reported after the age of 30 yrs, and fertility loss at an average age of 41 yrs [13, 14]. Yet many women, especially those in the workforce, tend to delay conception for education and a career. The chance for these women to have a successful pregnancy, however, is lower compared with younger women.

In vivo and _In vitro_ Fertilization

In human *in vivo* fertilization, the oocyte and sperm meet in the peritoneal cavity near the ovary or in the fallopian tube The sperm head penetrates the zona pellucida and binds and fuses with the plasma membrane of the oocyte Once the sperm enters the ooplasma, the oocyte rapidly undergoes a number of metabolic and physical changes called egg activation, including a rise in the intracellular concentration of calcium, completion of the second meiotic division and cortical reaction Chromatin from both the sperm and egg are then encapsulated in membrane-bound structures called pronuclei Over the next few days, the mammalian embryo undergoes a series of cell divisions forming a hollow sphere of cells called a blastocyst when the embryo moves into the lumen of the uterus on day 4 after ovulation The embryo will hatch out of the zona pellucida, attach to and penetrate the endometrium of the uterus on day 7 and grow there until birth But many factors may cause female or male infertility Female fecundity (conceiving ability) generally decreases with aging The monthly probability of an ongoing pregnancy for a 35-year-old (yo) is only about half of that of a 20-30-yo [15] Age-related infertility is considered to be resolvable with assisted reproductive technology

The birth of Louise Brown in 1978, the world's first "test tube baby" is a major milestone in the history of both medicine and science The "test tube baby" technique, *in vitro* fertilization (IVF) plus embryo transfer / transplantation, offers treatment to couples who previously had no hope of having a child of their own IVF was originally developed as an approach for overcoming mechanical blockage of fallopian tubes that prevented sperm from reaching and fertilizing ova released from the ovary However, this technique can be used for the treatment of infertility resulting from numerous causes, such as male sub-fertility and immune infertility

The IVF treatment cycle is a complex, multidisciplinary procedure A typical cycle for humans consists of the following phases

(1) Superovulation (ovarian stimulation) with a GnRH agonist or antagonist to suppress endogenous pituitary FSH and LH secretion, combined with stimulating folliculogenesis with FSH Human chorionic gonadotropin (hCG) is used to induce ovulation *In vitro* maturation of oocytes may be required for women with polycystic ovaries

(2) Oocyte retrieval by vaginal ultrasound-guided follicular puncture is followed by identification of oocytes

(3) *In vitro* fertilization or intracytoplasmic sperm injection (ICSI) with prepared sperm

(4) Identification of fertilized oocytes (zygotes) and further culture

(5) Evaluation and selection of embryos for transfer to the uterus [16]

Even though IVF techniques were developed and refined over the last three decades, the success rate of IVF clinics is still quite variable and depends on many factors including the laboratory and clinical approaches as well as patient characteristics such as age and physical uniqueness According to statistics from the Center for Disease Control and Prevention (CDC), the success rate of IVF clinics is 30-35% for women under age 35, 25% for women 35 to 37, 15-20% for women 38 to 40 and 6-10% for women over 40 [17] The positive association of unsuccessful pregnancy with age over 30 is largely due to spontaneous abortions [15], which may partly be due to the quality of ova IVF treatment with donor oocytes from younger women, however, may greatly enhance the reproductive prospects for women who have little chance to a successful pregnancy with their own oocytes [18] This highlights the age-related fertility decline in females as mainly, if not fully, driven by oocyte changes with aging All these studies suggested that the fertility rate of both *in vivo* and *in vitro* decline sharply after 35 yrs in humans The reproduction of aging women is still a big challenge even though assisted reproductive technology has made remarkable progress in the last 30 yrs

Mitochondria

Mitochondria are the energy center for cellular activity producing adenosine triphosphate (ATP) by aerobic respiration, which is the major source of energy in eukaryotic cells Mitochondrial size and shape vary with tissues and cells, typically they are sausage-like in shape with dimensions of 3-4μm in length and about 1μm in diameter [19] The morphology, size, quantity and distribution of mitochondria vary widely by organism, tissue type and different physiological conditions, even within the same cell types Under the electron microscope, mitochondria are double membrane-enclosed organelles with outer mitochondrial membrane (OMM), inner mitochondrial membrane (IMM), inter-membrane space (IMS) and matrix (Fig 2)

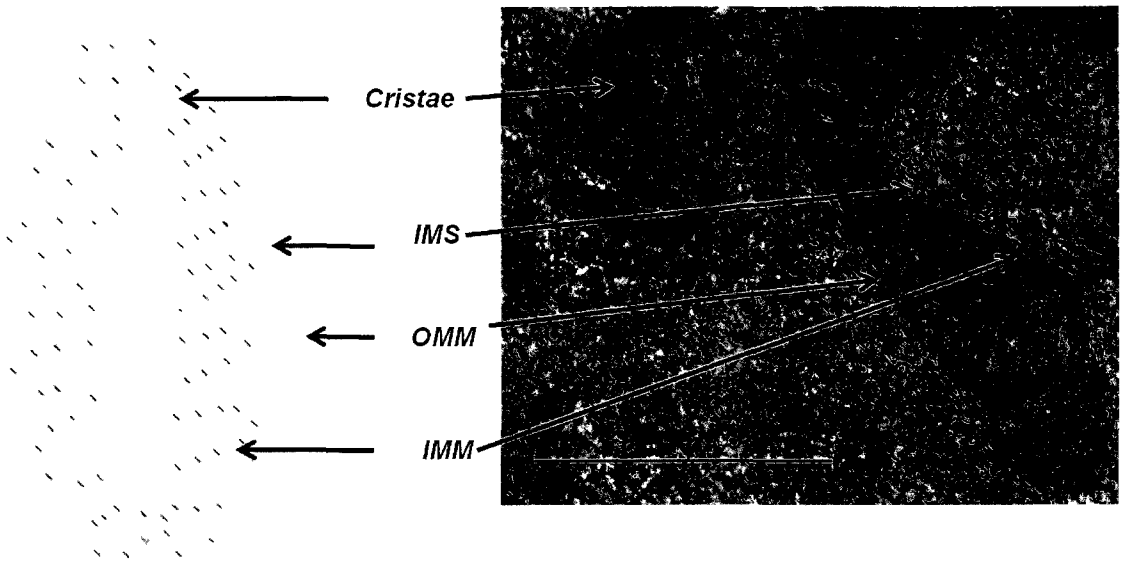

FIG. 2. Overview of a mitochondrion. Outer mitochondrial membrane (OMM), Cristae, inter membrane space (IMS) and inner mitochondrial membrane (IMM) (bar=500nm)

The outer membrane embeds some transport proteins and is permeable to small molecules, but large proteins need a specific signaling sequence to enter the inter-membrane space. The inter-membrane space is the space between the outer and inner membranes. The numerous cristae were thought to be the result of protruded IMM into a matrix, but after observation of three-dimensional images of mitochondria from electron tomography, Perkins et al. proposed that the continuity of the cristae with the inner mitochondrial membrane is achieved by a relatively small number of narrow tube-like connections [20]. In other words, the anatomical bottleneck can constitute a barrier and separate the two compartments: an intra-cristal space and inter-membrane space [21]. This view, however, is subject to debate [22]. The inner membrane is highly impermeable to all molecules. Many important proteins are on the inner mitochondrial membrane, such as proteins involved in the electron transport system, the ATP-synthesizing complex, fatty acid synthesis, and specific proteins for transport, metabolism, mitochondrial fusion and fission. Mitochondria are the most sensitive organelles to aging in the cell and may reflect the level of damage in a cell, such as DNA mutation, ATP deficiency, initiation of apoptosis and

necrosis. The role of mitochondria in apoptosis is very well established with support by many researchers [23-25]. Many studies suggest that mitochondrial dysfunction and mtDNA mutation may cause aging. Several studies have indirectly implicated mtDNA inheritance in longevity [26, 27]. Harman and others proposed a theory that mitochondria are the most relevant free radical target in aging besides being the main cellular source of reactive oxygen species (ROS) [28-30]. This theory provides an overview of the role of mitochondria in aging. Some mitochondrial characteristics contribute to the central role of mitochondria in aging, such as being the main ROS source and target, and the accumulation of mtDNA mutations and deletions from endogenous and exogenous factors causing phenotype resembling premature aging [31-33]. It is conceivable that exposure to certain environmental toxins and endogenous factors such as ROS could result in a preferential accumulation of mtDNA damage and accelerate aging [30, 34-37].

The electron transport chain (ETC) and ATP synthase are two of the most important structures in the mitochondrial inner membrane. The ETC couples electron transfer between electron donors (e.g., nicotinamide adenine dinucleotide (NADH) and flavin adenine dinucleotide ($FADH_2$)) and electron acceptors (e.g., O_2) to drive the transfer of protons out of the inner membrane. Complex I (NADH dehydrogenase) accepts electrons from NADH, and passes them to coenzyme Q (ubiquinone), which also receives electrons via $FADH_2$ electrons from complex II (succinate dehydrogenase)). Coenzyme Q passes electrons to complex III (cytochrome bc1 complex), which passes electrons to cytochrome c. Cytochrome c passes electrons to complex IV (cytochrome c oxidase, which reduces molecular oxygen to water). The mitochondrial electron transport chain is also one of the major cellular generators of ROS including superoxide (O_2^-), hydrogen peroxide (H_2O_2) and the free hydroxyl radical ($OH^\cdot$) [38, 39]. All of the electron carriers in the ETC could pass electrons to molecular oxygen, but coenzyme Q, namely the ubiquinone site in complex III and part of complex I are believed to be the two major ROS-forming sites [40-42]. ROS produced by mitochondria are believed to be an important factor in the aging process of many tissues and organs, such as brain and ovary.

Mitochondrial membrane potential

The ETC produces a mitochondrial membrane potential (MMP) across the inner

mitochondrial membrane MMP is formed by a proton gradient as a result of proton pumping by the oxidative respiratory chains located in the membrane [43] The concentration of protons in the IMS is much higher than in the matrix, since the inner membrane is impermeable to protons Thus an electrochemical proton gradient is established across both sides of the inner membrane This gradient is positive and acidic on the outside of IMM and negative and alkaline on the inside (matrix)

The proton gradient has two components a membrane potential and a pH gradient both driven by protons The energy stored in both the pH gradient and the membrane potential drives ATP synthase to synthesize ATP [44, 45] This mitochondrial membrane potential in most mammalian mitochondria is around 240mV [46] Regulation of MMP may play a functional role in cellular programs such as transport of metabolites and ions like calcium [47], importing of precursor enzymes [48, 49] and mitochondrial protein synthesis [50, 51] Changes of mitochondrial membrane potential may reflect different growing states or different phases in the cell cycle Darzynkiewicz et al suggest that MMP increases with the cell cycle moving from S to G2 to M phase [52], and different level of oxygen consumption may be accompanied by different MMP When cells begin to differentiate, MMP may also change [44] The MMP was reduced when erythroleukemia cells were induced to differentiate [53] The MMP is also the energy source driving outer and inner membrane fusion, a pH gradient is necessary for outer membrane fusion while an electrical potential is required for inner membrane fusion [54, 55], which are important for mitochondrial replication A decline of MMP suggests an increase of mitochondrial inner membrane permeability and a decreased proton gradient across the inner membrane, which will reduce ATP synthesis MMP disruption has been observed in many cases of necrosis and in more than fifty different models of apoptosis [56]

The mitochondrial membrane permeability transition pore (MPTP) is a high-conductance, non selective channel, which is assembled from the (1) pro- and anti-apoptotic members of the Bax and Bcl2 gene family, (2) mitochondrial outer membrane voltage-dependent anion ion channel (VDAC), (3) mitochondrial inner membrane adenine nucleotide (nt) translocator (ANT), (4) cyclophilin D, and (5) benzodiazepine receptor [57] The opening of MPTP channels occurs under

some pathological conditions such as stroke, traumatic injury and some neurodegeneration [58] VDAC, a member of the porin family, is a highly conserved protein located in the mitochondrial outer membrane Binding sites for hexokinase, glycerol kinase and Bax are located on the surface of VDAC Therefore those proteins are activators or inhibitors of MPTP Another protein of MPTP, ANT, is an inner mitochondrial membrane protein which can exchange adenosine diphosphate (ADP) and ATP between the mitochondrial matrix and the cytosol [59] Induced by pyridoxal phosphate, ANT can interact with VDAC and ADP/ATP on the binding site facing the cytosol In this case, the MPTP would open When the ADP/ATP binding site of ANT faces the mitochondrial matrix and ANT stops interacting with VDAC, the MPTP channel would close [60]

Most, but not all signals or stimuli that trigger overproduction of ROS and reduced MMP will activate the MPTP channel H_2O_2 out of mitochondria may interact with mitogenic signal transduction pathways, inhibit apoptosis by stabilizing the MPTP, and drive cell proliferation [61]

The opening of MPTP produces an increase of permeability of the mitochondrial inner membrane, leading to the collapse of the MMP, mitochondrial swelling and cell death Opening of MPTP is thought to be a consequence of apoptosis [62], but the opening of MPTP may result in release of apoptotic proteins stored in the mitochondrial inter-membrane space, specifically cytochrome c, procaspase-9, apoptosis initiating factor, and endonuclease G [63], which would promote apoptosis and provoke an apoptotic cascade reaction

Mitochondria also play an important role in regulating cytoplasmic calcium concentration with MPTP When the mitochondrial matrix is overloaded with calcium, MPTP will open to release Ca^{2+} into the cytoplasm from the matrix Conversely, when Ca^{2+} concentration in the cytoplasm is over the threshold limit, Ca^{2+} may enter mitochondria via Ca^{2+} channels Ca^{2+} can also be pumped back into the cytosol by a Na+/Ca^{2+} exchanger [64] Ca^{2+} overload and ROS generation can result in opening of MPTP channels [65], and the Ca^{2+} threshold for MPTP opening is coupled to irreversible increases in oxidative stress [66] The mitochondrial matrix is not homogeneous, but shows fine granularity of high electron density The intensity of high electron density varies with the metabolic state of the tissue observed The high electron density may be the result of sequestration and storage of calcium [67]

Mitochondria DNA (mtDNA)

Most genetic material is contained in the nucleus However, the mitochondrion is the only organelle with its own genome which is similar to bacterial genomes Mitochondria are thought to have evolved from bacteria [68] Mitochondrial DNA is maternally inherited because sperm mtDNA is degraded in the fertilized egg In mammals, mtDNA is a double-stranded circular mtDNA molecule with approximately 16 5kb including both heavy and light strands [21] The two strands of mtDNA are differentiated by their different guanine and thymine content and density in denaturing gradients The compact and contiguous circular mammalian mtDNA molecule does not have introns The genome contains 37 genes encoding two ribosomal RNAs (rRNA), 22 transfer RNAs (tRNA) and 13 polypeptides Some of the polypeptides are essential parts of the oxidative phosphorylation system The D-loop region on mtDNA contains the main regulatory sequences for transcription and replication initiation [69]

Peroxidative damage to nuclear and mtDNA or cell membranes has been considered the main mechanism for decay of cellular function by the free radical theory of aging [28] ROS including superoxide, H_2O_2, HOCl and others, are produced in mitochondria because of the leakage of high energy electrons through the electron transport chain The mtDNA is a major target of ROS, because (1) mtDNA is located near the inner mitochondrial membrane sites where oxidants are formed from the electron transport chain, (2) mtDNA lacks both protective histones and DNA repair ability unlike nuclear DNA [70], (3) mtDNA replication starts from a D-loop with a single strand, which produces some mutant genome from "replication jumping" by removal of any single-stranded "excess" DNA up to a double-stranded region [71]

Mitochondria and oocyte aging

Egg production, maturation, fertilization and embryo development are factors which define the quality of an oocyte [72] Oocyte production and maturation consist of nuclear and cytoplasmic replication and maturation Fertilization and embryo development require both nuclear and cytoplasmic maturation in the oocyte [73] The release of the first polar body marks nuclear maturation, while cytoplasmic maturation is more complicated Evaluation of mitochondria has been suggested as a useful estimate of cytoplasmic maturation [74]

Mitochondrial replication occurs in parallel with increasing cellular metabolism. Thus, the increasing ATP needs are matched by increasing mitochondrial numbers which is generally associated with increasing cytoplasmic volume. In mice, the number of mitochondria expands 10,000 times in immature oocytes progressing from the primordial follicular stage to mature ovulated oocytes [75]. The human metaphase II (M II) oocyte is estimated to have 100,000 to 200,000 mitochondria. Maximum mitochondrial size and cristae complexity are reached just at the beginning of the phase of rapid oocyte growth and decline thereafter in humans [76]. As human oocytes age, mitochondria accumulate mtDNA mutations after decades of exposure to ROS and other free radicals, which may reduce mitochondrial ATP generation [77]. The development of primordial follicles was found to be delayed or arrested with lower ATP supply [78].

Many age-related functional and morphological changes occur in oocytes which include increased density of the mitochondrial matrix, increased ROS production, increased mtDNA mutations, decreased MMP and decreased ATP synthesis [79, 80]. The adult resting primordial follicular oocyte has about 6000 mitochondria on average [75]. The total germ-line mitochondrial number will decrease to 5 million in 800-1,000 germ cells by puberty and will continue to fall [81].

The MMP is related to oocyte aging in many ways. The age-related decrease of MMP in human oocytes and embryos was observed by Wilding [82]. This reduction may be caused by a decrease of ANT, an important protein of MPTP [83]. High-polarized mitochondria are required in the pericortical oolemma for ATP production and calcium homeostasis [84] which is necessary for sperm penetration and cortical granule exocytosis [85]. Low ATP levels caused by low MMP may also limit energy for oocytes and pre-implantation embryos [86, 87]. The ATP produced by mitochondria is critical for nuclear and cytoplasmic maturation of oocytes [88] and sustaining the activity of the meiotic Ca^{2+} wave pacemaker [89]. Therefore, low-polarized mitochondria may be one of the major reasons for poor fertility of aged oocytes. Mitochondria also contain anti-apoptotic and apoptogenic components such as cytochrome c. Apoptosis of oocytes from aging mice also increases and this correlates with their observed increase of abnormalities in oocyte mitochondria as well [90]. Apoptosis may be one of the protective mechanisms to eliminate damaged oocytes with accumulated mtDNA mutation [91].

The apoptotic rate of old immature oocytes (from 41-50-yo women) is significantly higher than young oocytes (from 21-40-yo women) and consequently the developmental potential of oocytes from older women decreases sharply [92]. ROS is one of the reasons for the high apoptotic rate in old oocytes. Thouas [86] suggested that excessive ROS production in aged oocytes might promote the opening of MPTP and subsequently initiate the release of cytochrome c, which activates the mitochondrial caspase apoptotic cascade pathway. The process may contribute to preimplantation embryo arrest [86]. Opening of VDAC may induce apoptosis by releasing cytochrome c. Blocking VDAC1 activity in bovine oocytes with anti-VDAC1 antibodies resulted in the change of physiologically maturing oocytes *in vitro* [93]. Oocytes are more susceptible to mitochondrial dysfunction since mtDNA does not replicate until postimplantation [94], which may restrict replication of mitochondria. The mtDNA copy number varies in oocytes, and aging exerts a negative influence on the process of mitochondrial genesis [95].

Compared with young oocytes, aged oocytes also produce a higher proportion of embryos with normal appearance but abnormal genes, such as chromosomal aneuploidy [96]. Abnormal motor proteins may contribute to aneuploidy in aged oocytes [97], while polo-like kinases, spindle assembly regulators, need ATP as one of the phosphate donors for phosphorylation [98]. Therefore, lower ATP or MMP levels may contribute to chromosomal aneuploidy in aged females, which is probably part of the mechanism of age-related mitochondrial dysfunction on abnormal oocyte spindle assemblies [99-101].

Mitochondrial distribution may be used as one marker to estimate cytoplasmic maturation. An oocyte in the germinal vesicle stage shows homogeneous mitochondrial distribution throughout the ooplasma [82], while oocytes in metaphase I (M I) or M II generally show heterogeneous mitochondrial distribution with a peripheral pattern. Most M II oocytes have large granulated mitochondria clumped in the pericortical cytoplasm [78]. Mitochondrial redistribution in different cellular zones is conducted by the cytoskeletal microtubules [102]. The improper formation of the cytoplasmic microtubule network contributes to abnormal distribution of mitochondria (such as homogenous mitochondrial distribution in M II oocytes), which leads to inappropriate ATP distribution and contributes to retardation or arrest of embryogenesis [103]. Distribution of

mitochondria not only influences ATP distribution, but also affects the regulation of calcium The demand for ATP and calcium provoke mitochondrial redistribution in oocytes [104] Mitochondrial aggregation with smooth endoplasmic reticulum (SER) in mature oocytes is essential for their cooperation on regulating calcium concentration In mammals, activating oocyte development by sperm fertilization initiates a prolonged series of elevations of intracellular Ca^{2+}, which is generated by increasing production of inositol 1,4,5-triphosphate (IP3)[105] Sperm fertilization initiates IP3 production by introducing some sperm factors into the oocyte, such as sperm-specific phospholipase c, which is the primary candidate for the elevation of Ca^{2+} [106-108] Oocyte maturation not only requires a high level of ATP production, but also needs proper regulation of calcium concentration in the cytoplasm, mitochondria matrix and SER [74, 104] Calcium performs an important role in the embryonic cellular cycle and establishment of the embryonic axis [109]

Mitochondria from cumulus cells versus mitochondria from platelets

Some groups have introduced mitochondria from autologous cumulus cells into oocytes [110, 111] However, because of age-related mitochondrial defaults in cumulus cells, autologous cumulus cell mitochondrial microinjection is not the best option Studies have shown that the incidence of deletion of mtDNA 4,977bp (Δ4,977) in granulosa cells was positively associated with aging [112, 113] Use of platelets as the mitochondrial source has the following two benefits (1) platelets degenerate in about 10 days in the circulatory system if they are not involved in clotting [114] This rapid turnover of platelets results in reducing defective mitochondria and defective mtDNA platelet load [115] (2) Platelets are anucleate, thus excluding nuclear DNA contamination of the autologous mitochondrial microinjection into oocytes

Hamster oocytes and reproduction

In hamsters, the first set of follicles mature just prior to the first ovulation occurring between 26-30 days of age[116] In addition to hormone influence, hamster oocyte ovulation is also determined by the time of lights-on during a 24 hr period [117] More than 12 5 hr of light per day are required for hamsters [118] Constant light interferes with ovulation, but does not block development of follicles [119]

The female hamster reproductive cycle is invariant in length at four days On day 2 of the

cycle, each ovary contains 10-12 follicles whose antral cavities expand rapidly between late day 3 and early day 4 About 50% of the oocytes in large follicles ovulate between late day 4 and early day 1, while the other 50% become atretic [120] In the four-day cycle, estrogen levels increase and plateau over day 3 to early day 4, reaching peak by noon of day 4 Progesterone levels peak in the afternoon of day 4, the same with FSH and LH So ovulation occurs between late day 4 to early day 1 [121]

Hamsters are an excellent animal model for the study of oocytes, microinjection and fertilization for several reasons (1) hamster ova are less fragile than mouse ova, which in our laboratory, leads to more successful microinjected hamster ova, (2) the hamster ovum is closer to the human ovum not only in durability but also in size (about 100μm) (3) female hamsters show a regular and predictable four-day estrous cycle, (4) large numbers of eggs (30-60) can be obtained from superovulation, and (5) in-house production of hamsters is convenient with 16 days of gestation and around 10 pups born per liter [122]

The same age-related decline of fertility occurs in hamsters as in humans Mizoguchi reported that the fertilization rate in aged hamsters decreased and suggested that defective ova were one of the major factors resulting in increased preimplantation loss in aged hamsters [123] Successful IVF in the golden hamster was reported in 1964 [124] After decades of development, IVF in hamsters became a mature and usable technique for research But even though the hamster is a good model for reproductive research, the hamster has not been used in much research on age-related changes of oocytes and age-related mitochondrial changes in hamster oocytes have not been extensively studied to date Therefore, we have used the hamster as our model to (1) analyze age-related mitochondrial changes in the oocyte, (2) to improve mitochondrial function in oocytes and (3) improve the fertility of hamster oocytes by introducing mitochondria from autologous platelets into aged oocytes If this works in hamsters, we predict that in the future, some older women with infertility due to aging ova would seek similar methods to improve their fertility

All of these studies suggest dysfunction of mitochondria is one key factor contributing to oocyte *in vivo* aging Therefore we proposed that replacement of mitochondria in aged oocytes with healthier mitochondria may be a reasonable treatment to retrieve oocyte function

SPECIFIC AIMS AND APPROACHES

1 To test the hypothesis that mitochondria of oocytes from young hamsters have significant morphological and functional differences compared to those from old hamster Individual ovaries and oocytes were recovered from young (2-4 month) and old (12-14 month) female golden Syrian hamsters We evaluated perivitelline space of oocytes in young compared to old hamsters by light microscope (oocytes without perivitelline space are deemed to be healthy oocytes [125]) We compared mitochondrial quantity changes in oocytes from young and old hamsters by MitoTracker green fluorescence staining and measurement of mtDNA copy number, and compared quality change by ATP level, ROS and JC-1 fluorescence staining We also used TEM (Transmission Electron Microscopy) to evaluate mitochondrial quantity and quality (ultrastructure) of oocytes from young and old hamsters

2 To test the hypothesis that platelet mitochondria from young hamsters are not significantly different compared to those from old hamsters We compared the mitochondrial quantity, quality and ultrastructure of platelets from young and old hamsters by mtDNA copy number, ATP level and TEM

3 To test the hypothesis that mitochondrial quantity and function can be improved by introducing "young" autologous mitochondria into old oocytes Copy number of mtDNA, density of MitoTracker fluorescence and ATP level were measured to analyze mitochondrial quantity and quality change in oocytes between pre- and post-microinjection of autologous mitochondrial suspensions derived from autologous platelets Oocytes and platelets were isolated from both young and old hamsters Platelets from a superovulated female were isolated from blood drawn from the inferior vena cava (IVC), and the mitochondria were isolated from those platelets Following this exsanguination, excised fallopian tubes were irrigated to collect the superovulated ova Autologous mitochondria were microinjected into experimental ova from

each superovulated young and old female hamster while sham control ova were microinjected with the carrier substance only.

4. To test the hypothesis that oocyte fertilization can be improved by introducing "young" autologous mitochondria into old oocytes. Control (non-injected), sham-control and microinjected ova were co-incubated for four hours with sperm collected from healthy young male hamsters. The resulting embryos were evaluated daily for development to the blastocyst stage.

SIGNIFICANCE

The significance of my research lies in the possibility and practicability of introducing healthier, autologous mitochondria into an aging hamster oocyte to improve fertilization and embryo production rates. This approach might then be applied to human oocytes obtained from older women.

CHAPTER II

AGE-RELATED MITOCHONDRIAL CHANGES OF HAMSTER OOCYTES

INTRODUCTION

Many age-related mitochondrial changes in oocytes have been reported about human, mouse, rat and pig [10, 103], but few of them are about hamster Here, we plan to prove that there are some defects of mitochondrial quantity and quality in oocytes from old hamsters compared to those from young hamsters Therefore in this chapter, ATP levels, mtDNA copy number, ROS level and MMP were determined in oocytes from young and old hamsters Transmission electron microscopy was performed to evaluate oocyte ultrastructure

MATERIALS AND METHODS

Female golden Syrian hamsters were grouped into a young hamster group (2-4 months) and an old hamster group (12-16 months) according to Parkening's classification [2] The animals were housed in a temperature and light controlled room All experimental protocols and animal handling procedures were reviewed and approved (#07-016 and #10-035) by the Institutional Animal Care and Use Committee (IACUC) of Old Dominion University (ODU) All of the reagents and materials were purchased from the companies listed in Table 3-5

Statistical analysis

The data were analyzed by using the Statistical Package for Social Sciences (SPSS) 18 0 program The percentage of blastocyst formation was evaluated by using a χ^2 test The perivitelline space of oocytes was tested with Student's t-test after transformed to arcsine The relationship between ATP content and mitochondrial DNA copy number in an oocyte was evaluated by using the Pearson correlation test The ATP content, mitochondrial copy number, ratio of dark mitochondria and fluorescence intensity of oocytes from young and old hamsters were compared with Student's t-test The ATP content, mitochondrial copy number and fluorescence intensity of oocytes from control, sham and microinjected group were compared one-way Analysis of Variance (ANOVA) followed by comparison among groups The results are presented as mean ±SD, and $p<0\ 05$ was considered statistically significant

Superovulation

Old female hamsters selected at random with regard to estrous were induced to super-ovulate by intra-peritoneal (IP) injections of Pregnant Mare's Serum Gonadotropin (PMSG) followed 54 hours (hrs) later by hCG Super-ovulated females were sequentially euthanized over a period of 2 hrs starting approximately 17 hrs after the hCG injection

Collection of Superovulated Metaphase II Oocytes

Animals were anesthetized with 0 2 ml of 60 mg/ml sodium pentobarbital by IP injection and the experiment began 2 minutes (min) later The abdominal area was sterilized with 70% ethanol The abdomen was entered by creating a small hole over the umbilicus and then stripping the skin simultaneously down over the hind legs and up over the forelegs Oviducts were excised (salpingectomy) by first gently stretching and then shredding the mesosalpinx and mesometrium close to each oviduct and uterine horn, respectively, and then cutting between the oviduct and the ovary at the intramural junction with microsurgical scissors Oviducts were placed in sterile 35x5 mm polystyrene Nunclon culture dishes with 3 ml of M199TE medium as described by Yamauchi et al [122] Under a Zeiss dissecting stereomicroscope at 20x magnification, watchmaker forceps were used to slide the fimbrial os onto a 26-gauge sterile needle attached to a 1 ml sterile syringe A cumulus oophorus cell with oocyte complex (COC) was irrigated from the oviducts with medium expressed from the syringe with moderate force COC from individual hamsters was placed in a 100 µl 1% hyaluronidase / medium mixture under paraffin oil and evaluated continuously for the cumulus cells to dissociate from the oocytes Oocytes that were close to being cell-free were then picked up with a hand-pulled glass micropipette (approximate 100 µm lumen inner diameter) and washed 3 times through hyaluronidase-free medium with vigorous pipetting to remove all cumulus cells Normal M-II-stage eggs (judged by minimal perivitelline space with one small polar body pressed against the oolemma) were evaluated at 32x magnification and collected from the 4th wash droplet to a Petri dish with medium for the experimental protocols

Some of the normal M-II-stage oocytes were collected at 32x magnification from the 35mm dish and each oocyte was transferred with 3 µl medium into cryotubes with 97 µl somatic cell ATP

releasing reagent and immediately frozen with liquid nitrogen as oocyte lysate for ATP and mtDNA analysis.

Evaluating Oocyte Perivitelline Space

All ovulated oocytes were counted. Those oocytes which were expanded tightly against the zona pellucida (minimal perivitelline space) with a clear indentation at the polar body (Fig. 3) were judged to be healthy oocytes [125]. Oocytes with a wide perivitelline space were judged poor in quality and discarded.

Fluorescence Labeling Mitochondria and Confocal Microscopy

Fluorescence Labeling Mitochondria with JC-1

The potential-sensitive fluorescence dye 5,5',6,6'-tetrachloro-1,1,3,3'-tetraethylbenzimdazoylcarbocyanine iodide (JC-1) was used to measure the activity of mitochondria by reflecting MMP. The process was performed according to a previously described method [86]. Low-polarized mitochondria with MMP (negative inside) between neutrality and 100 mV generally show green fluorescence under the confocal or fluorescence microscope because of the monomer form of JC-1. High-polarized mitochondria (MMP $\geq$ 140 mV) are indicated by red fluorescence due to JC-1 aggregate formation. The stock solution was 0.77 mM in dimethyl sulfoxide (DMSO). Before use, the dye was diluted in M199TE to 1μM as the final working solution at room temperature. The retrieved oocytes were incubated in the JC-1 working solution for 30 min at 37° according to the description of Zeng et al. [78]. The fluorescence was evaluated under a Zeiss LSM-510 confocal laser scanning microscope equipped with a Kr-Ar laser to produce an excitation wavelength of 488 nm, and a 530 nm dichroic mirror was used to allow passage of the emission wavelength. The emission wavelength was analyzed by a photomultiplier after being filtered through a 527~538 nm band-pass filter (green emission) or 581~602 nm filter (red emission). A Z-section scan with 5 μm intervals through the center of the oocyte was used for the analysis of fluorescence intensity as described by Van Blerkom et al. [126]. The images were processed and the intensities of both red and green fluorescence of JC-1 in the oocyte were measured by using MetaMorph 7.5.

Quantification of ROS and mitochondria in oocytes

Intracellular ROS was quantified with MitoTracker Red CM-H_2XROS (MRR) MRR is oxidized by ROS, mainly by superoxide and hydrogen peroxide and trapped in mitochondria by its chloromethyl moiety [127] The total mitochondrial population was measured by labeling mitochondria with MitoTracker Green FM (MGF) MGF covalently bind to mitochondrial proteins by reacting with free thiol groups of cysteine residues [128] Experiments were performed in a similar way to the steps of JC-1 staining above The stock solutions of MGF and MRR were each 1 mM in DMSO The final working solutions were 400 nM and 1 μM in M199TE respectively Emitted fluorescence from MGF and MRR passed through 535 and 600LP emission filter A Z-section scan with 5 μm intervals through the center of the oocyte was used for the analysis of fluorescence intensity

Quantification of ATP

The content of ATP in individual oocytes was determined by the ATP bioluminescent somatic cell assay kit based on the luciferin-luciferase reaction A volume of 100 μl of 1 5 diluted ATP assay mix was added to individual wells in a white opaque 96-well plate and kept at room temperature for 3-5 min to allow endogenous ATP hydrolysis One hundred μl ice-cold somatic cell ATP-releasing reagent and 50 μl of ultrapure water were mixed with 50 μl sample or standard 100 μl of the mixture were transferred to one of the duplicated reaction wells in the 96-well plate with 100 μl ATP assay reagent diluted 1 5 The amount of light emitted from every reaction well was immediately measured using a Dynex MLX microtiter plate luminometer The background luminescence was subtracted from readings of all wells The ATP in single oocyte samples was calculated by comparison to a standard curve generated over the range of 2 5-500 fmol/100 μl

Real-time polymerase chain reaction (quantitative PCR or QPCR) quantification of mtDNA in oocyte

QPCR using the Roche Lightcycler 480 system was used to quantify mtDNA copy numbers PCR primers were designed using the mitochondrial 12S ribosomal DNA sequences for golden hamster by LightCycler Probe Design Software 2 0, and synthesized by Integrated DNA Technologies, Inc Hamster 12S ribosomal DNA primer sequences were

5'TCAAAGGACTTGGCGG3' (forward) and 5'CTTCCAGCCCATAGG3' (reverse). The specificity of selected primers was tested by conventional PCR (1 cycle of denaturation at 95°C for 4 min, 35 cycles of amplification at 95°C for 30 sec, 55°C for 30 sec, 72°C for 30 sec and 1 cycle of extension at 72°C for 1 min), and the length of PCR products was measured by electrophoresis. The 12S mitochondrial ribosomal DNA amplicons (192 bp) were subcloned into pCR2, a TOPO-cloning vector. Recombinants were isolated, purified plasmid DNA was obtained using a Qiagen Plasmid Isolation kit according to the manufacturer's instructions, and the inserted mtDNA sequence was confirmed by DNA sequence analysis. The purified plasmid DNAs (pFCHam12S) were quantified by spectrophotometry at 260 nm. DNA concentration (μg/μl) was calculated from OD 260 value and plasmid concentration was obtained by dividing DNA concentration by plasmid molecular weight.

Recombinant plasmid DNA was used to construct the standard curve in order to quantify the mitochondrial genomes (mtDNA) in the same oocytes used for the ATP assay. The circular nature of the recombinant substrate was expected to more accurately reflect the topology of the endogenous mtDNA and produce more reliable amplification [129].

The LightCycler DNA FastStart SYBR Green kit was utilized to perform QPCR. Two μl of oocyte lysate (as described in the method of collection of superovulated M II oocytes) was used as a template in a 20 μl final volume, including 0.2μM each of the forward and reverse primers, 2mM $MgSO_4$ 4 μl SYBR mix. In the positive and negative control capillaries, 2 μl 10^7 purified pFCHam12S plasmid solution as positive control and water as negative control replaced oocyte lysate respectively. All sample capillaries, positive and negative, were duplicated for reliable data. The DNA was denatured at 95°C for 10 min, then amplification proceeded for 45 cycles at 95°C for 0 sec, 55°C for 5 sec and 72°C for 12 sec, followed by melting curve analysis to detect mis-priming. A standard curve from 10 – 10^8 DNA molecules was generated by serial 10-fold dilutions with water of the appropriate purified stocks of pFCHam12S. Relative mtDNA copy numbers for individual oocytes were calculated by comparison to the standard curve established previously.

Oocyte Preparation for Transmission Electron Microscope

TEM preparation used modified procedures described by Brittion et al. [130]. Oocytes collected above were fixed in 2.5% glutaraldehyde (GA) in 0.1 M phosphate buffer (PB) for 4 hrs at 4°C. Subsequently, oocytes were washed twice in 0.1M PB, once in 10% bovine serum albumin (BSA) in Dulbecco's PBS (Phosphate buffered saline) and transferred to a Beem capsule (flat bottom size 3) containing 1 drop of 10% BSA. Following a 30 min rest, the capsules were spun in a swinging bucket centrifuge for 15 min at 1800g. Three drops of GA were carefully overlaid on the surface of the BSA to avoid mixing. The capsules were centrifuged horizontally for 1 hr again and subsequently filled with GA and refrigerated at 4°C overnight. On the following morning, the GA was poured off and the fixed protein/oocyte mold was transferred from the Beem capsule to a 1 ml vial. The mold was washed twice in 0.1M PB and post-fixed with osmium tetroxide (1% osmium tetroxide in 0.1M PBS) for 2 hrs and then washed twice in PB. The mold was dehydrated in ethanol gradients (30%, 50%, 70%, 90%, 95%, 10 min each and 2x 100%, 15 min each) and infiltrated with pure propylene oxide 2x for 15 min each. Then the mold was infiltrated in 1:1 EMBed 812 mixture and propylene oxide for 1 hr and pure EMBed 812 for 1 hr sequentially. The EMBed 812 mixture was made from an Embed 812 kit with 20ml EMBed 812, 9ml DDSA (dodecenyl succinic anhydride), 12ml NMA (Methyl-5-Norbornene-2,3-Dicarboxylic Anhydride), and 0.75ml DMP-30 (Dimethylaminomethyl phenol). The mold was aligned into a Beem capsule filled with EMBed 812 mixture and polymerized in a 60°C oven for 48 hrs. The samples were cut on an RMC-MT2C ultramicrotome. Thin sections were collected on G200-Cu grids, stained with uranyl acetate and lead citrate sequentially, and examined on a JEM-1200EXI electron microscope.

RESULTS

Evaluating Perivitelline Space of Oocytes

Young and old hamsters were superovulated and oocytes were dissociated from cumulus masses. Of 522 oocytes from 14 young hamsters, 88.68 % were predominantly expanded against the zona pellucida (minimal perivitelline space) with a clear indentation at the polar body (Fig. 3), which are judged to be healthy oocytes [125, 131], while 58.64% of 322 oocytes from 17 old

hamsters could be described in this way. The remaining old oocytes had wide perivitelline spaces with no indentation from the polar body. The data reveals that young hamsters produced more morphologically healthy-appearing oocytes (88.68%) in comparison to old hamsters (58.64%), which is an age-related significant decrease of 33.87% in percentage of healthy oocytes from aged vs. young hamsters (p=0.00015, Student's t-test with arcsine transform, p=0.00015) .

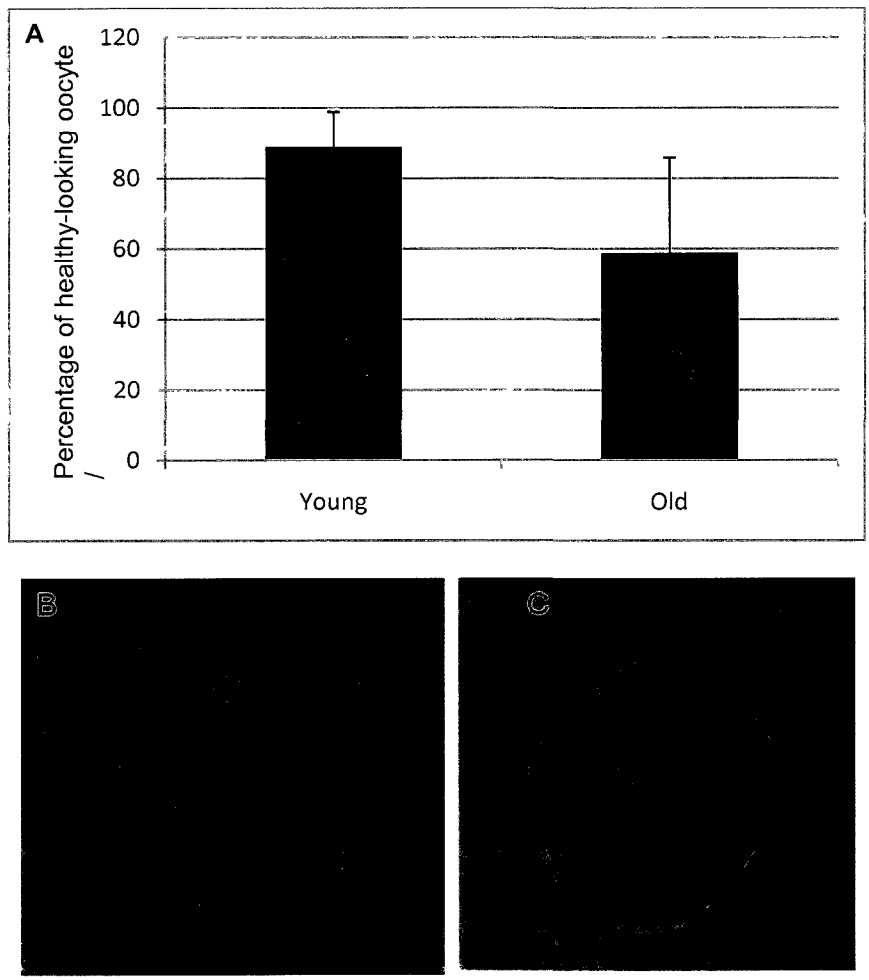

FIG.3. Morphological difference between oocytes from young hamster vs. old hamster. **A)** Young hamsters have a significantly higher number of "healthy-appearing" oocytes vs. old hamsters. Approximately **B)** 88.68% of young oocytes were expanded against the zona pellucida with a clear indentation at the polar body in comparison to 58.64% in old oocytes. **C)** The remaining old oocytes had wide perivitelline spaces with no indentation from the polar body 522 from 14 young hamsters and 322 from 17 old hamsters).

Polarization of mitochondria in M II oocytes from young and old hamsters

The green and red fluorescence intensities of JC-1 in M II oocytes were measured by MetaMorph 7.5. The green fluorescence intensity of oocytes from young hamsters was similar (Student's t-test, P=0.561) to those from old hamsters, and the red fluorescence intensity of oocytes from young hamsters was significantly higher (Student's t-test, P=0.002) than those from old hamsters (Fig. 4A). The young oocytes had a significantly higher (Student's t-test, P=0.014) ratio of red/green fluorescence intensity (6.9) of JC-1 than old oocytes (4.3) (Fig. 4B).

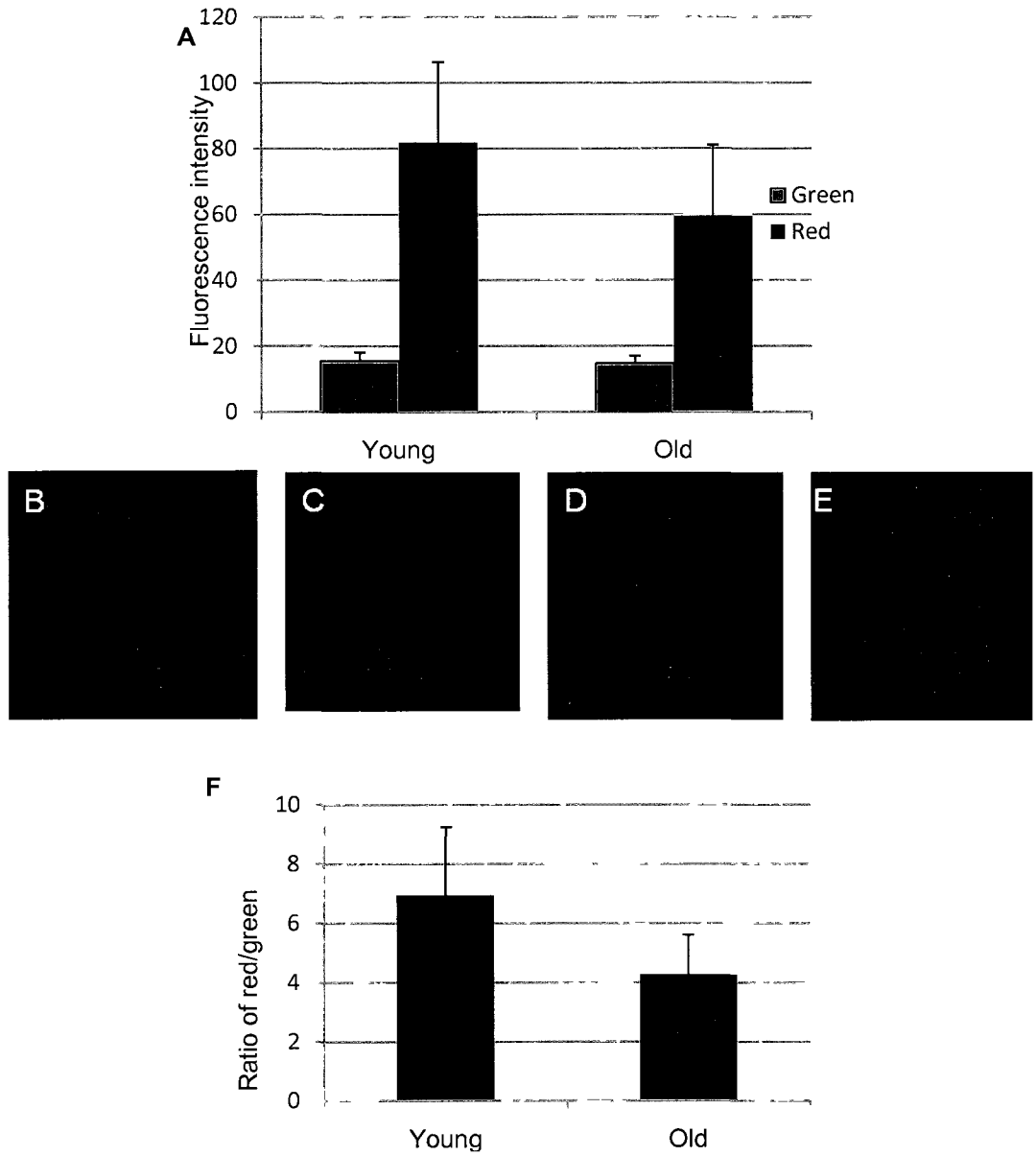

FIG.4. Fluorescent signals in JC-1 stained oocytes. **A)** Intensities of green(**B)** for young and **D)** for old) and red(**C)** for young and **E)** for old) fluorescence. **B** to **E)** are image samples of oocytes. **F)** Mean ratio of red/green relative fluorescence of JC-1 stained M II oocytes (n=24 for young from 5 hamsters, n=30 for old from 6 hamsters) from young and old hamsters. The red fluorescence intensity of oocytes from young hamsters was higher (P=0.002) than those from old hamsters, and young oocytes had higher (P=0.014) red/green fluorescence intensity ratio than old oocytes. The data are presented as mean ±SD.

The reactive oxygen species (ROS) level in M II oocytes from young and old hamsters

MitoTracker Red CM-H_2ROS was originally developed to stain mitochondria [132]. MRR may be used to determine the intracellular quantity of ROS [133]. Cytoplasmic fluorescence intensities of MGF staining images were analyzed with software MetaMorph 7.5. The oocytes from old hamsters incubated with MRR showed a significant increase (Student's t-test, P=0.049, n=30) in ROS production compared with those from young hamsters (Fig. 5).

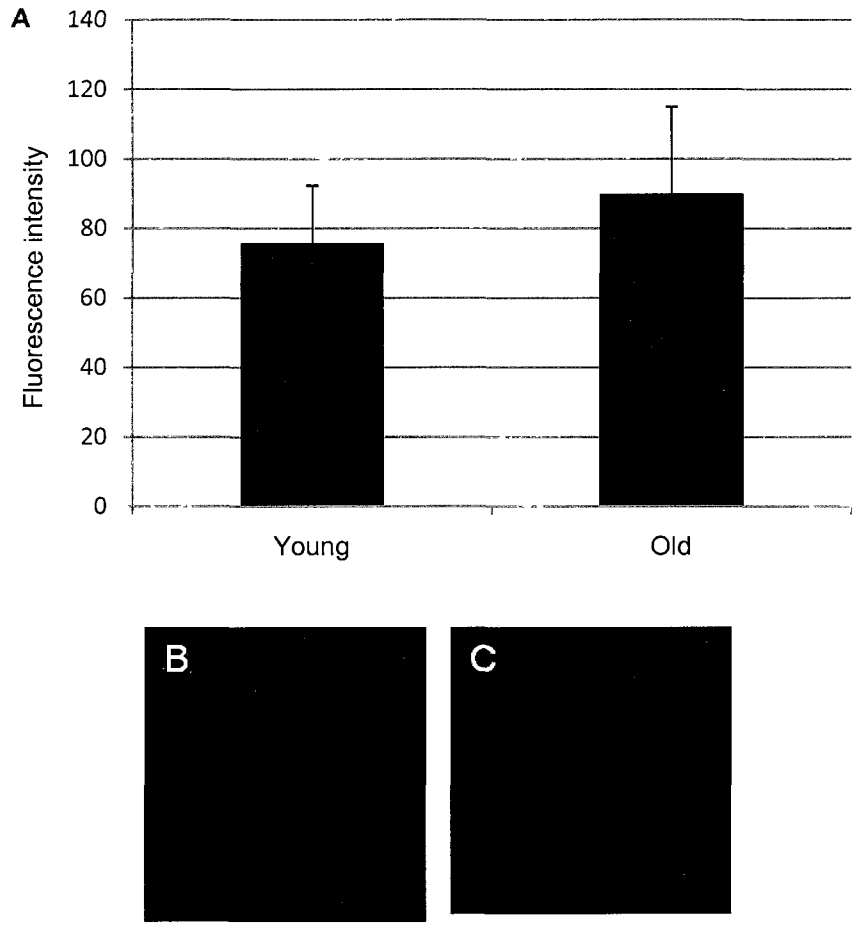

FIG.5. Fluorescent signals of oocytes stained with MitoTracker Red CM-H2XROS. **A)** The intensities of fluorescence of oocytes from old hamsters stained with MitoTracker Red CM-H2XROS are significantly higher than those from young hamsters (p=0.049, n=30 in each group from 6 young and 6 old hamsters). **B)** and **C)** are image samples of young and old oocyte respectively. The data are presented as mean ±SD.

Quantification of mitochondria labeled with MitoTracker Green FM

MitoTracker Green FM is a fluorescence dye which can specifically bind to mitochondria. A comparison between the fluorescence intensities of oocytes from young and old hamsters is presented in Figure 6. Cytoplasmic fluorescence intensities of MGF staining images were analyzed with MetaMorph 7.5. As shown in Figure 6, no significant difference was seen between young and old oocytes (Student's t-test, n=30, p=0.08).

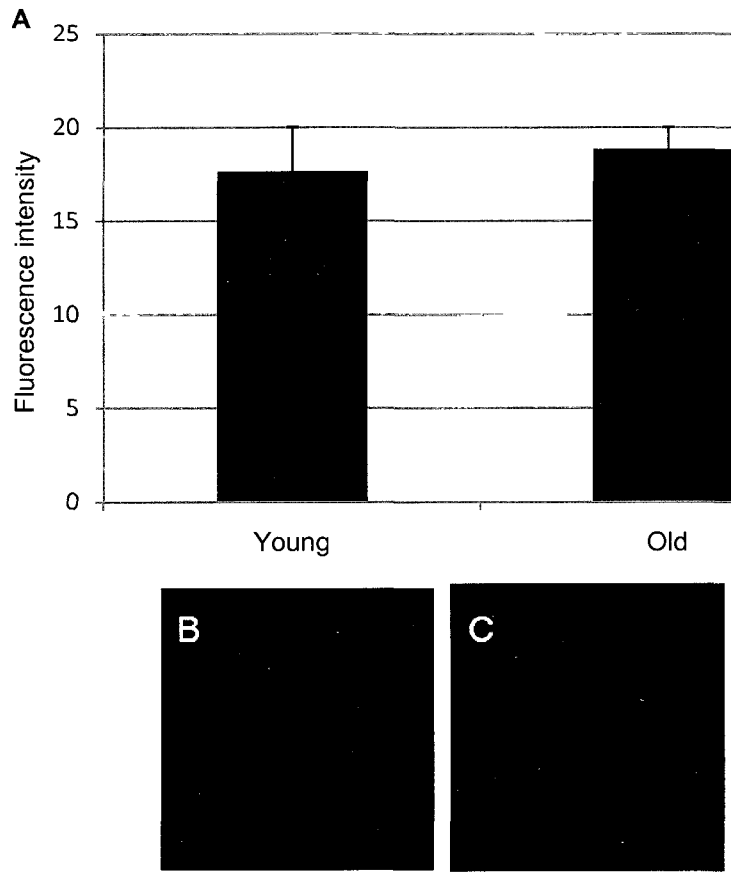

FIG.6. Fluorescence signals of oocytes stained with MitoTracker Green FM. **A)** The intensities of fluorescence of oocytes form old hamsters stained with MGF are not significantly different with those from young hamsters (p=0.08, n=30 in each group from 6 young and 6 old hamsters). **B)** and **C)** *are image samples of young and old oocytes respectively. The data are presented as* mean ±SD.

Quantification of ATP

As one of the mitochondrial functional measurements, the levels of intracellular ATP in individual oocytes from young (2-4 months) and old (12-16 months) hamsters were determined. ATP levels were measured in 163 hamster oocytes (90 from 6 young hamsters and 73 from 7 old hamsters). The average ATP level in oocytes from old hamsters (78.45 ±80 fmoles /oocyte) was significantly lower (Student's t-test, p=0.002) than those from young hamsters (121.5 ±94 fmoles /oocyte) (Fig.7). This represents a decrease of 35.4% in the average level of ATP in old hamster oocytes compared to that in young hamster oocytes.

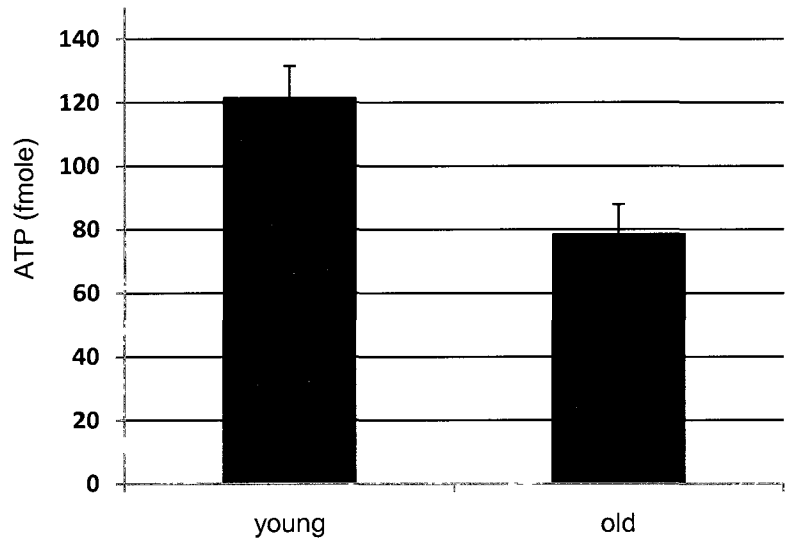

FIG.7. ATP content in oocytes from young and old hamsters. Average ATP level in oocytes from young hamsters (121.5 ±94 fmoles /oocyte) was significantly higher (p=0.002) than those from old hamsters (78.45 ±80 fmoles /oocyte). 163 hamster oocytes were measured for ATP level, 90 from 6 young hamsters and 73 from 7 old hamsters The data are presented as mean ±SD.

Real-time polymerase chain reaction (PCR) quantification of oocyte mtDNA

Mitochondrial DNA is present at about 100,000 copies per mature oocyte, with 2 copies per mitochondrion on average [134, 135]. As shown in Figure 8A, 118 hamster oocytes (63 from 7 young hamsters and 55 from 7 old hamsters) were retrieved and mtDNA content was measured by real-time PCR. Young hamsters contained an average of 8.3 ±8 $x10^4$ mtDNA copies while an average of 4.1 ±6.4 $x10^4$ copies were found in old oocytes; a decrease of 51.8% (Student's t-test, p=0.0015) in the average number of mtDNA genomes in old hamster compared to young hamster oocytes.

Correlation of ATP Levels and mtDNA Number in Individual Hamster Oocytes

Figure 8B indicates significant linear relationship between the ATP levels and the mtDNA numbers in hamster oocytes when the average values are compared with Pearson correlation test. In addition, Figure 8B also shows that there is a medium (r=0.311) correlation of ATP level and mtDNA number within individual hamster oocyte (p=0.007). These correlations suggest that a low number of mitochondrial genomes, and hence mitochondria, results in a low level of ATP per oocyte, whether that oocyte is from a young or old hamster.

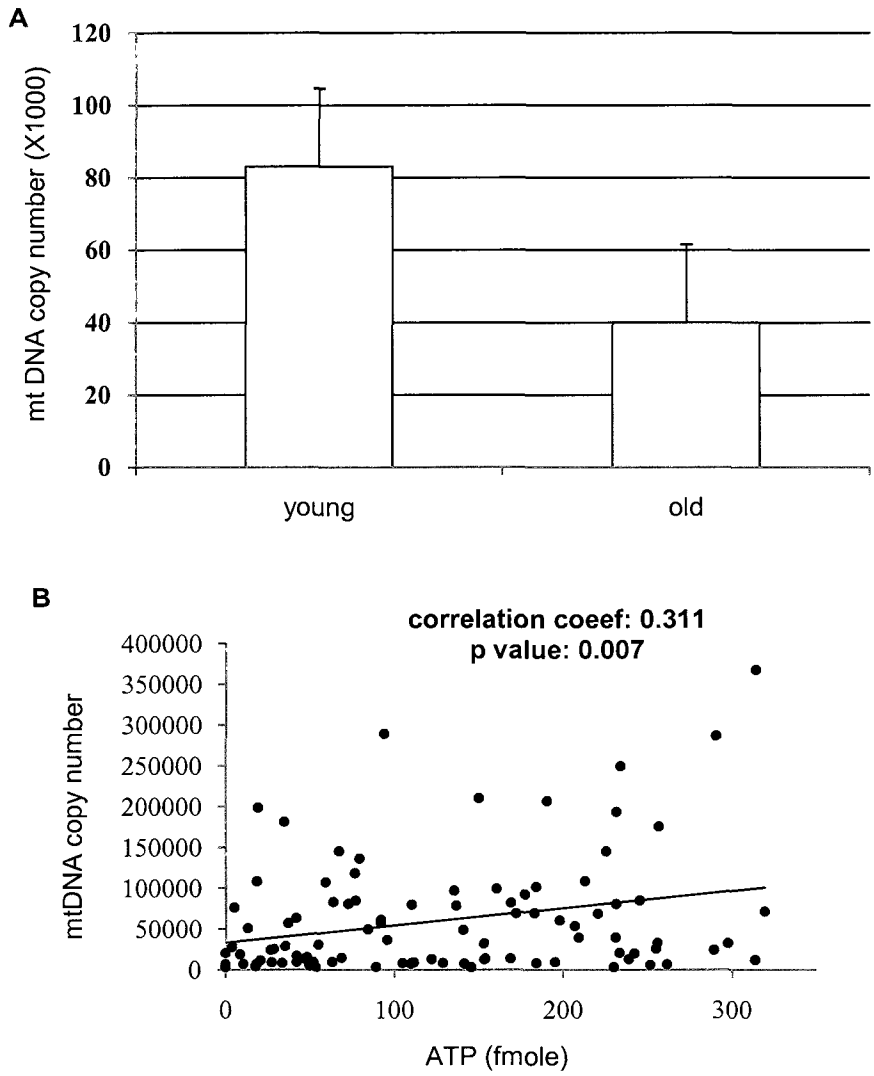

FIG.8. MtDNA content and relationship between mtDNA and ATP contents in oocytes. **A)** Young hamsters contained an average of 8.3 ±8 $x10^4$ mtDNA copies while an average of 4.1 ±6.4 $x10^4$ copies were found in old oocytes, (ANOVA, p=0.0015). 118 hamster oocytes (63 from 7 young hamsters and 55 from 7 old hamsters) were measured for mtDNA copy number. **B)** A medium (r=0.311) correlation of ATP level and mtDNA number was found within individual hamster oocytes, (Pearson correlation test p=0.007). The data are presented as mean ±SD in Figure A .

Mitochondrial morphological difference between young and old hamster oocytes by TEM

Figure 9 shows examples of mitochondrial morphological differences between oocytes from young and old hamsters The independent experiments represent 6 young and 6 old female hamsters Figure 9A and 9B show young (A) and old (B) hamster oocytes at 2,000 x A statistically significant decrease of 36% (p=0 0000041, Student's t-test with arcsine transform), in mitochondrial number in aged vs young individual hamster oocytes, and data are presented in Table 1 Figure C and D show young (C) and old (D) hamster oocytes at 10,000 x All oocytes contain some dark mitochondria with large amounts of electron dense areas but old oocytes on average contain a significantly higher frequency (31% higher) of dark mitochondria without distinct cristae (Student's t-test, p=0 0002), and data are presented in Table 2 E and F show collapsed cytoplasmic lamellae in higher magnification within old oocytes (F), but these were not seen in young oocytes (E) The analysis was performed with ImageJ with Plugins downloaded from the National Institute of Health (NIH) contributed by Alberto Duina and Tseng Qingzong et al , following the method as described by Weibel et al [136]

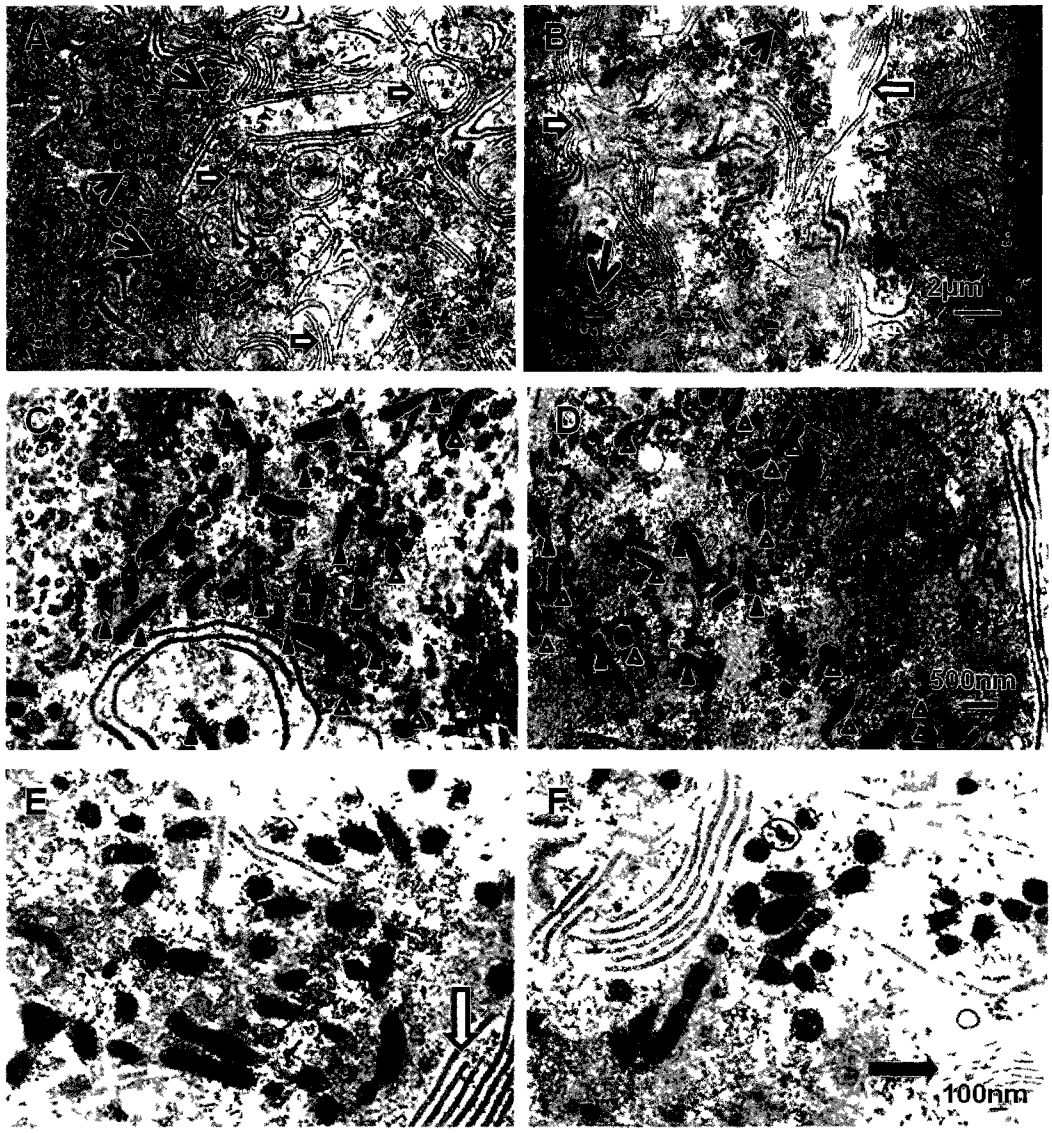

7

FIG 9 Mitochondrial morphological examples of oocytes from young and old hamsters **A)** Young and **B)** old oocytes at 2,000 x Note mitochondria (➔), normal cytoplasmic lamellae (⇨) Significantly higher mitochondrial number in oocytes from young hamsters (p=0 0000041) **C)** Young and **D)** old oocytes at 10,000x Note dark mitochondria (Δ), mitochondria with clear cristae (▲) All oocytes contain some dark mitochondria with large amounts of electron dense areas but old oocytes display significantly higher frequency of dark mitochondria without distinct cristae(p=0 0002) Collapsed cytoplasmic lamellae (⟶) in **F)** old oocytes, but not in **E)** young oocytes at 19,000x The independent experiments represented 6 young and 6 old female hamsters

TABLE 1. Number of mitochondria per visual field in oocytes from young and old hamsters.

Subject	Young group	Subject	Old group
Y1-1	81	O1-1	55
Y1-2	81	O1-2	42
Y1-3	90	O2-1	45
Y1-4	88	O2-2	74
Y1-5	81	O2-3	50
Y2-1	67	O2-4	42
Y2-2	109	O2-5	53
Y2-3	79	O3-1	51
Y2-4	65	O3-2	53
Y2-5	86	O3-3	50
Y2-6	62	O4-1	75
Y2-7	74	O4-2	90
Y3-1	77	O4-3	58
Y3-2	60	O4-4	60
Y4-1	61	O4-5	52
Y5-1	60	O5-1	64
Y6-1	78	O6-1	53
Y6-2	74	O6-2	46
Y6-3	66	O6-3	54
Y6-4	71	O6-4	41
Mean	75.5		55.4

TABLE 2. Number of dark mitochondria and mitochondria with clear cristae per visual field in oocyte of hamsters.

Young group				Old group			
Subject	Mc	Md	Mc/(Md+Mc)%	Subject	Mc	Md	Mc/(Md+Mc)%
Y1-1	16	20	44.4	O1-1	9	12	42.9
Y2-1	17	16	51.5	O2-1	6	12	33.3
Y2-2	13	13	50.0	O2-2	3	7	30.0
Y2-3	14	10	58.3	O2-3	4	7	36.7
Y3-1	21	14	60.0	O3-1	10	16	38.5
Y3-2	14	7	66.7	O3-2	11	16	40.7
Y3-3	8	6	57.1	O3-3	7	10	41.2
Y4-1	5	6	45.5	O4-1	25	35	41.7
Y4-2	11	8	57.9	O5-1	41	54	43.2
Y4-3	13	9	59.1	O6-1	25	41	37.9
Y4-4	11	7	61.1				
Mean			55.6	Mean			38.6

Dark mitochondria without clear cristae(Md), mitochondria with clear cristae (Mc)

DISCUSSION

Mitochondrial morphological and functional age-related changes in human and mouse oocytes have been reported by many groups [10, 103], but rarely reported for the hamster. Only Mizoguchi et al.[123] reported that defective oocytes with chromosomal abnormality represent one major factor leading to increased preimplantation loss in the aging hamster. Large perivitelline spaces were related to lower fertilization rates [131] in humans. We evaluated morphological differences between young and old oocytes by light microscopy. We found old hamsters produced a significantly lower percentage (33.87% lower) of healthy-appearing oocytes with minimal perivitelline space than young hamsters. This result coincided with the lower fecundity rates of old female hamsters compared with that of young ones according to previous research [123].

Oocyte quality has been associated with the size of the mitochondrial population [137]. Oocyte energy comes mainly from mitochondrial ATP, so healthy mitochondria are needed in sufficient numbers to maintain the ATP level necessary for oocyte development and fertilization. The amount of mtDNA can accurately reflect the quantity of mitochondria. In humans the average mtDNA in fertilizable oocytes is 250,454 copies, while oocytes that do not fertilize have an average

mtDNA copy number of 163,698 [138]. We have also shown that mtDNA number decreased significantly in M-II-stage oocytes from old hamsters compared with those in young hamsters. Even though we don't know the mitochondrial threshold for successful fertilization of a hamster oocyte, the 51.8% decrease of mtDNA in old oocytes is one of the main factors contributing to the low fertility rate of the aging hamster. There are large standard deviations of the mtDNA copy number, which may come from the physical uniqueness of individual hamsters. Therefore, nested ANOVA may be used here for avoid bias of individuals.

Ultrastructural evaluation of mitochondria further confirmed the significant difference of mitochondrial number between oocytes from young and old hamsters. As shown by TEM pictures in Table 1, oocytes from young hamsters contained a 36% higher average number of mitochondria than those from old hamsters.

MitoTracker Green FM was also used to semi-quantify mitochondria. The mitochondria in oocytes were labeled with MitoTracker Green in Figure 6. However, the result is controversial compared with QPCR data. The data show no significant difference between young and old oocytes. Combined with our JC-1 data, the nonconformity between MitoTracker Green and mtDNA results could be explained by the possibility that MitoTracker Green is partly a mitochondrial membrane potential dependent dye. MitoTracker Green is supposed to selectively accumulate in the mitochondrial matrix where it covalently binds to mitochondrial proteins by reacting with free thiol groups of cysteine residues [128]. It should stain mitochondria with green fluorescence regardless of mitochondrial membrane potential according to the manuals. However, MitoTracker Green fluorescence intensity has been demonstrated to be both MMP and oxidation sensitive [139]. Therefore, MitoTracker Green may not have been a good choice for membrane potential independent analysis of mitochondrial quantity due to this probe's sensitivity to both MMP and oxidation [140]. Alternatively, immunohistochemistry or immunofluorescence could be used as a complementary method to further confirm mitochondrial quantity in future research.

From the mtDNA and TEM data, we saw that on average the young oocytes had more mitochondria than the old oocytes. Mitochondrial quantity and quality are both important for

oocyte development and fertilization. Therefore, the following mitochondrial functional measurements were performed to identify possible points of malfunction in old oocytes.

MMP is one of the most important and common mitochondrial functional indices. A decrease in MMP reflects mitochondrial dysfunction and is related to increases in a series of mitochondrial functional changes such as ROS production, decreased ATP level and irregular calcium regulation. Here we report the first published evidence about MMP changes in hamster oocytes. Based upon the increased red fluorescence by JC-1 stained oocyte (Fig. 5A), young oocytes have higher polarization of their mitochondria than do old oocytes. To remove the bias from the difference in mitochondrial quantity between young and old oocytes, we used the ratio of red-to-green fluorescence intensity to reliably describe this change. Figure 5B demonstrates the ratio of red/green fluorescence intensity to be significantly lower in oocytes from old hamsters. According to the characteristics of JC-1, this ratio implies that a higher percentage of the mitochondria in young oocytes maintain a higher polarization than those in old oocytes which are highly polarized. Since the energy stored in the mitochondrial membrane potential drives ATP synthase, the polarization reduction in old oocyte mitochondria could lead to a reduced ATP production, which is observed in Figure 8A. It remains to be determined if decreased MMP is an inducer or a subsequent event in the apoptotic pathway, but in either case, the decrease in MMP indicates the possibility of increased apoptosis occurring in older oocytes. This decrease in MMP could be related to the poor development of old oocytes and low fecundity of old hamsters.

Another index of mitochondrial dysfunctional index is ROS levels. Our data show that ROS levels in old oocytes are significantly higher than in young oocytes. This data suggests the accumulation of defective mitochondria with higher ROS concentrations in the oocytes from old hamsters. Conflicting reports have been published on the changes in MMP and ROS generation [141]. Some studies show mitochondrial uncoupling as a cytoprotective strategy to limit ROS generation, while other authors think collapse of MMP induces ROS generation [142, 143]. The relationship of ROS production to apoptosis has been well documented and we propose that our demonstrated increase in ROS production contributed to mitochondrial dysfunction as well. The

apoptosis assay, such as measurement of active caspases, should be used in the future to support this.

Evaluation of morphological changes in mitochondrial ultrastructure indicated that old oocytes manifested a higher frequency of dark mitochondria without distinct cristae. Old oocytes possessed more mitochondria with high density and less mitochondria with distinct cristae than young oocytes. Our hamster oocyte morphology agrees with the increase in cristae complexity and electron density seen in the mitochondrial matrix with both *in vivo* and *in vitro* human oocyte aging [76]. Mitochondrial morphology changes with follicular development. Weakley reported that the electron density of the mitochondrial matrix and the complexity of cristae increased in the rapidly enlarging oocyte until follicular antral formation and declined thereafter [144]. Thus the electron density in our TEM partly reflects the mature level of oocytes. Ishida et al. suggested that high electron density may be the result of sequestration and storage of calcium [67].

The density changes in mitochondria are intimately associated with the smooth endoplasmic reticulum (SER) [144]. Our TEM micrographs did not reveal changes in regular vesicle SER, but we observed some cytoplasmic lamellae (CL). CL are a conformational change in the SER [145] and collapsed forms of these structures were observed only in oocytes from old hamsters. The abnormalities of both CL and mitochondria together might indicate a dysfunction in the regulation of calcium concentration in the cytoplasm and mitochondrial matrix, since mitochondria and SER play important roles in tittering calcium concentration.

The data presented in this chapter illustrate both mitochondrial dysfunctions and morphological changes in oocytes from old hamsters vs. young hamsters. These parameters probably contribute to a lower fertility rate and fecundity through decreased ATP production, abnormal regulation of calcium concentration and transfer, and increase of ROS in addition to other mechanisms that are not yet elucidated.

CHAPTER III

COMPARISON OF PLATELET MITOCHONDRIAL STRUCTURE AND FUNCTION BETWEEN YOUNG VS. OLD HAMSTERS

INTRODUCTION

Transfer of both ooplasm and autologous cumulus cell mitochondria into aging oocytes in humans and mice has been reported by some groups [110, 111, 146, 147]. However, mitochondrial heteroplasmy was barred by the Food and Drug Administration (FDA) [146], and age-related accumulation of mtDNA defects in cumulus cells weakened the reliability of these two methods. Therefore, we chose platelets as our source of mitochondrial transfer because of the rapid turnover rate and anuclearity. In this chapter, ultrastructure and ATP levels in platelets from young and old hamsters were compared to test these hypothesized advantages of platelets for mitochondrial transfer.

MATERIALS AND METHODS

Recovering platelets

Hamsters were injected with 0.1-0.2 ml sodium pentobarbital depending on body weight (60mg/ml in 10% ethanol, 20% glycerol, 70% water), followed by a midline incision along the linea alba to open the abdomen. The IVC was exposed and a Surflo 16Gx2" IV (intra-venous) catheter was inserted into the IVC. An anticoagulant solution of heparin (0.2 ml) was injected into the IVC prior to blood withdrawal with a 5 ml (6 ml capacity) syringe. About 4.0 ml blood was transferred to a 5 ml test tube with 0.5 ml anticoagulant citrate/dextrose solution. After that, 1.5 ml Histopaque was placed into a 10 ml Accuspin tube and centrifuged at 1,700g for 30 seconds to spin the Histopaque below the frit (a porous high density polyethylene barrier which separate tube into two chambers) of the Accuspin tube. Blood (4.5 ml) from IVC of hamster was transferred into the Accuspin tube and spun at 1,000g for 10 min to separate the platelet-containing plasma layer from leukocytes and erythrocytes in the blood. The plasma layer was transferred into a new 15 ml tube filled with 12 ml of Eagle's minimum essential medium (MEM). The tube was spun at 1,700g for 15 min. The pellet was re-suspended in 4.5 ml MEM and spun at 1,700g for 15 min again. The supernatant was aspirated to yield the final pellet which was re-suspended in 200 µl somatic cell

ATP releasing reagent and immediately frozen with liquid nitrogen and stored in -80°C freezer for ATP and mtDNA analysis.

Quantification of ATP

The platelet lysate was diluted 1:500 with 998 µl pure water after thawing to produce the working solution for ATP and mtDNA analysis. Preliminary experiments showed that the concentration of this working solution was in the reliable range of the standard curve mentioned above. The ATP content in the platelet lysate from 40 µl of blood, using 100 µl of platelet-lysate working solution, was determined by the ATP bioluminescent somatic cell assay kit with the same protocol used in oocyte lysate analysis described in Chapter 2. The amount of light emitted was measured using a Dynex MLX micro-liter plate luminometer.

Real-time PCR quantification of mtDNA

The LightCycler DNA FastStart SYBR Green kit was utilized to perform real-time PCR in the same protocol used for measuring mtDNA of oocyte lysate. Two µl of platelet lysate was used in a 20 µl final volume with duplication. Two µl of 10^7 purified pFCHam12S solution and water were used as positive and negative controls respectively. A standard curve from 10 to 10^8 mtDNA molecules was generated by serial 10-fold dilutions of the appropriate purified stocks of pFCHam12S. Relative mtDNA copy numbers for individual oocytes were calculated compared with the standard curve.

Platelet Preparation for Transmission Electron Microscope

Platelet preparation for TEM was performed in the same manner as oocyte preparation for TEM described in Chapter 2.

RESULTS

Ratio of ATP to mtDNA in platelets from young and old hamsters

Platelets have an average of 4 mitochondria and each mitochondrion contains a single mtDNA molecule [148]. Therefore, the ratio of ATP content to mtDNA molecules reflects ATP level per mitochondrion and suggests mitochondrial function in platelets. As shown in Figure 10, 1,000 platelet mitochondria from young hamsters produced an average of 40.4 ±48.4 fmoles ATP molecules, compared with an average of 33.4 ±47.8 fmoles ATP molecules per 1,000 platelet

mitochondria from old hamsters. This difference was not significant (Student's t-test, p=0.72). Blood samples were drawn from 12 young and 14 old hamsters. This result suggests that platelets from young and old hamsters have similar ATP levels.

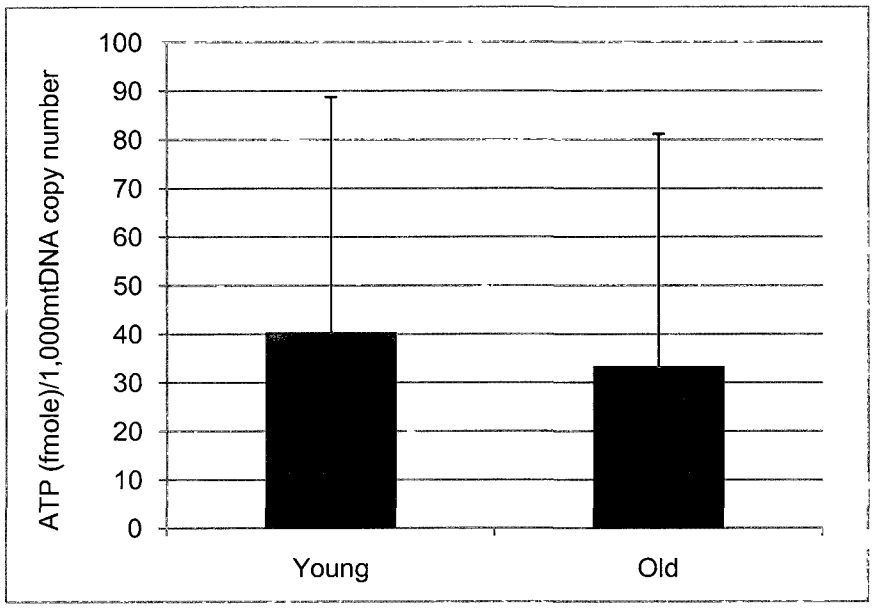

FIG.10. Ratio of ATP molecule number per 1,000 mtDNA molecules in platelets from young and old hamsters. An average of 40.4 ±48.4 fmoles ATP molecules per 1,000 mtDNA molecules was produced from platelet mitochondria from 12 young hamsters compared with an average of 33.4 ±47.8 fmoles ATP molecules from platelets from 14 old hamsters. No significant difference was observed (p=0.72).

Mitochondrial morphology of platelets

The ultrastructure of platelet mitochondria did not show obvious differences between young and old hamsters. The cristae of platelet mitochondria (Fig 11A and 11B) were not as clear as mitochondria from other somatic cells such as cumulus cells (Fig 11C), and there were more electron-dense particles in the platelet mitochondria. This characteristic of platelet mitochondria was similar to mitochondria in oocytes.

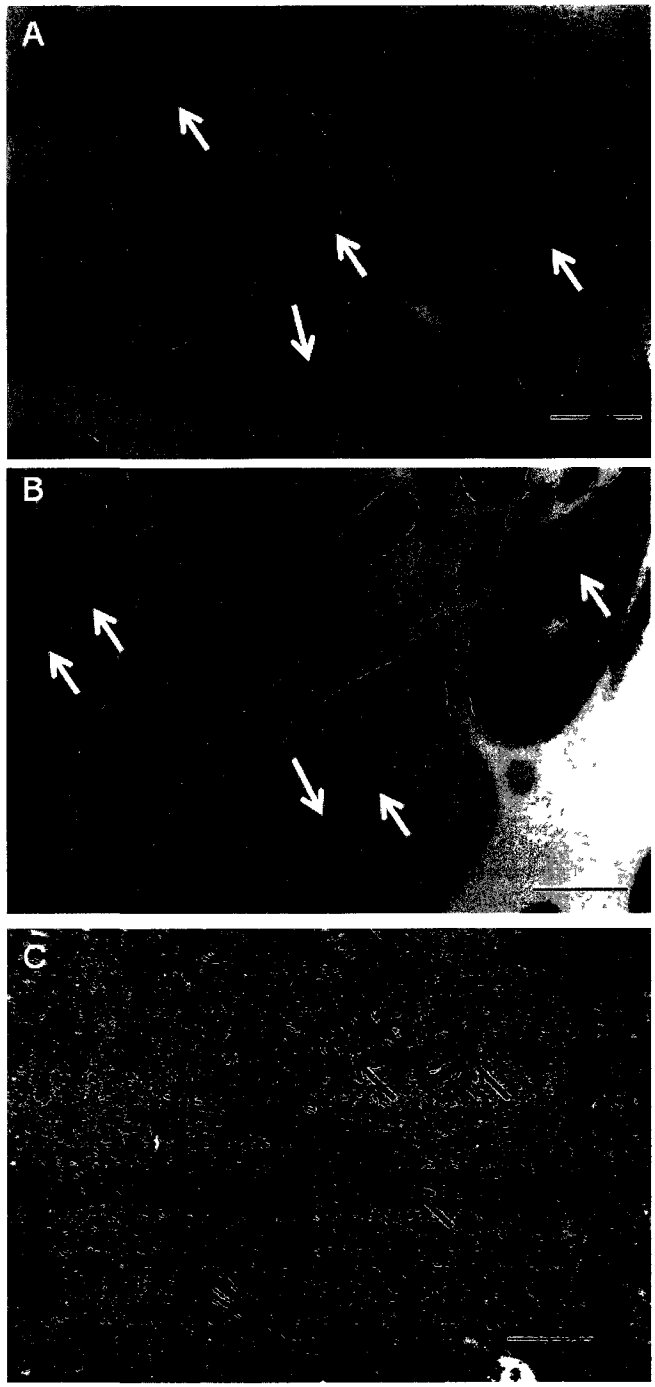

FIG.11. Mitochondrial morphology of platelets. The ultrastructure of platelet mitochondria does not show obvious differences between **A)** young and **B)** old hamsters. The cristae of platelet mitochondria were not as clear as mitochondria from other somatic cells such as **C)** cumulus cells, namely there were more electron-dense particles in platelet mitochondria. The white arrows point to mitochondria in platelets. The dark arrows point to mitochondria in cumulus cells.(Bar=500nm)

DISSCUSSION

Ooplasmic transfer and autologous cumulus cell mitochondrial transfer to aging oocytes have been reported in humans and mice [110, 111, 147] However, since the mitochondria with their own mtDNA come from different individuals, ooplasmic transfer may leads to heteroplasmic embryos The heteroplasmic embryos with heterogenous mtDNA constructed showed highly variable levels of heteroplasmy in different tissues [149] and among offspring [81] Heteroplasmy may produce problems involving mitochondrial-related diseases, because haplogroup and sub-haplogroup defining changes may affect mitochondrial replication [150] In addition, the ethical problem of heterogeneous genetic material is hard to overcome Consequently, this procedure has been rejected by the FDA [146]

Some types of age-related mtDNA mutations, such as deletion of 4,977bp on mtDNA (Δ4977), have also been reported in platelets of aging humans [151-153] The 4977bp deletion is a common deletion of mtDNA and generally causes some sporadic mitochondrial related diseases such as Pearson's syndrome and Kearn-Sayre syndrome It occurs between two 13-bp direct repeats at positions 13447-13459 and 8470-8482, and has been used as a mtDNA damage biomarker [154] Cumulus cells also contain some age-related mutations such as deletion of 4,977bp on mtDNA The frequency of Δ4977 in cumulus cells from women over 34-yo are two times higher than those women below 34-yo (6 9% vs 3 2%, [113]) The aged cumulus cells with high frequency of mitochondria with Δ4,977 in are not appropriate for mitochondrial transfer The frequency of Δ4,977 in human platelets, however is below 0 00018%, much lower than other cell types [115]

From the data above, no significant difference was found between morphology and ATP production of platelets from young and old hamsters The ratio of ATP molecules to mtDNA molecules means the energy production level per platelet mitochondrion can be considered an accurate reflection of mitochondrial function This result suggested that platelet mitochondria from old hamsters were as good as those from young hamsters in ATP production Therefore, platelet mitochondria were chosen here for autologous mitochondrial transfer We did not measure mtDNA mutation of platelets, but it is assumed that the rapid turnover of platelets (about 10 days)

probably filters most of the defective mtDNA out of the platelet mitochondrial cohort according to previous description [115]. Detection of platelet mtDNA defects and additional measurements of mitochondrial function and morphological changes can be performed in future research to further confirm the similarity between platelet mitochondria from young and old hamsters.

With the critical advantages of platelets, including anucleate condition and rapid turnover rate, platelets can be considered as the better source (with normal ATP production) of autologous mitochondrial transfer. In addition, the relative high electron density of the platelet mitochondrial matrix is similar to that of oocytes from Figure 11 and other reports [155]. This similarity may benefit oocytes more than autologous mitochondrial transfer from other tissues and cells.

CHAPTER IV

MITOCHONDRIAL CHANGES IN HAMSTER OOCYTES FOLLOWING AUTOLOGOUS PLATELET MITOCHONDRIAL MICROINJECTION

INTRODUCTION

After confirming the age-related mitochondrial changes in oocytes from old hamsters and the desirable characteristics of platelets as a source for mitochondrial transfer, all M II oocytes collected were divided into three groups -- control (un-injected), sham-injected and microinjected groups. For sham injections, the injection pipette was introduced into the oocyte without injecting any foreign material. For microinjection, the injection pipette was introduced into the oocyte and autologous platelet mitochondria in M199 media were injected into the oocyte. ATP level and mtDNA copy number were determined respectively within individual oocyte of the three groups. MitoTracker Green FM was used to further estimate the quantity of mitochondria.

MATERIALS AND METHODS

Collection of Superovulated M II Oocytes

All protocols followed the methods outlined in Chapter II. All M II oocytes collected here were divided into three groups- control, sham injection and microinjection groups.

Recovering platelet mitochondria

Platelets were isolated following the protocol given in Chapter III but stopped before lysis in somatic ATP releasing reagent.

Mitochondrial isolation

The platelet pellet was transferred to a 1 ml micro-centrifuge tube, suspended in isotonic buffer ST20 [156] (Table 3) followed by homogenization with the Dounce homogenizer. The sample was placed in a Parr Cell Disruption Bomb for further platelet disruption at 1200 psi for 20 min on ice prior to rapid decompression. The resultant suspension was centrifuged at 1000g at 4°C for 10 min to pellet the un-broken platelets. The resulting supernatant was transferred into another 1 ml micro-centrifuge tube and centrifuged again at 5000g for 15 min at 4°C. The

mitochondrial pellet was finally suspended in 20 µl M199TE, and this mitochondrial suspension was transferred under oil to a square petri dish for microinjection

Autologous mitochondrial transfer by microinjection

A square petri dish (containing several 150 µL M199TE droplets with one oocyte each and the mitochondrial suspension droplets) was overlaid with mineral oil (density 0 84 g/ml) The micromanipulation injection system consists of a (1) PLI-100 pico-injector with a Thomas Ultra Air Pac air compressor, (2) Nikon Diaphot light microscope that has a hanging ICSI micromanipulation apparatus mounted with a microinjection pipette (4 micron tip diameter, 60 mm length, 30°angle) and (3) holding pipette (9-17 micron tip diameter, 60 mm length, 30°angle) A 10-15 pl aliquot of mitochondrial suspension was drawn into the ICSI pipette The oocyte, on the holding pipette, was injected with mitochondrial suspension through the zona pellucida and oolemma into the ooplasm After incubation for 1 hr, some oocytes were transferred with 3 µl M199TC into a cryotube with 97 µl somatic cell ATP releasing reagent and immediately frozen with liquid nitrogen before storage in -80°C freezer for ATP and mtDNA analysis The other oocytes were incubated with 400 nM MGF for fluorescence labeling of mitochondria Oocytes in the sham injection group had an empty needle inserted into the ooplasm for 5 seconds

Quantification of ATP and Real-time PCR quantification of mtDNA in oocytes

All protocols were identical to the methods used in Chapter II

Mitochondrial Fluorescence Labeled with MitoTracker Green FM and Confocal Microscopy

All protocols were identical to the methods used in Chapter II

Counting mitochondria in pellet with real-time PCR and TEM

The pellet of mitochondria was suspended in 20 µl M199TE, The number of mitochondria in this mitochondrial suspension was counted by real-time PCR with the same method described in Chapter II, since there are 1~2 mtDNA in each mitochondrion The result of real-time PCR was confirmed by TEM The mitochondria in each TEM picture were counted The number of mitochondria in each picture was considered as the number of mitochondria in the volume of picture area times 0 5µm since the average size of mitochondria is 0 5-1µm The total number was obtained by comparing the volume of picture area timing 0 5µm and the volume of pellet

RESULTS

Real-time PCR quantification of mtDNA in oocytes from the three groups

As shown in Figure 12, 74 old hamster oocytes (29 control , 21 sham , and 24 microinjected) were retrieved, injected and measured by real-time PCR. Control Oocytes contained an average of 6.8 ± 8.8 $x10^4$ mtDNA copies, sham oocytes contained an average of 7.5 ± 10.6 $x10^4$ mtDNA copies, and microinjected oocytes contained an average of 8.0 ± 16.8 $x10^4$ mtDNA copies. No significant increase (One-way ANOVA, p=0.92) in mtDNA occurred due to sham or mitochondrial microinjection compared with the control group.

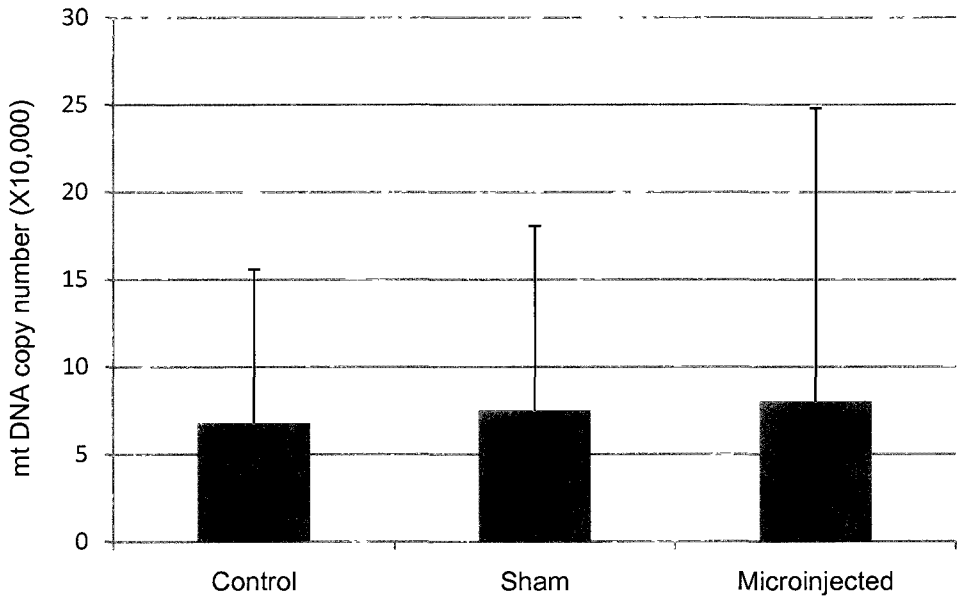

FIG.12. Quantification of mtDNA in oocytes from control, sham and microinjected groups. 74 old hamster oocytes (n=29 of control, 21 of sham, and 24 of microinjected) were retrieved, injected and measured by rtPCR. Control oocytes contained an average of 6.8 ±8.8 $x10^4$ mtDNA copies, sham oocytes contained an average of 7.5 ±10.6 $x10^4$ copies, and microinjected oocytes contained an average of 8.0 ±16.8 $x10^4$ copies. The experiments represented 7 old female hamsters. The data are presented as mean ±SD.(P>0.05)

Quantification of ATP in oocytes from control, sham and microinjected groups

In order to check the mitochondrial functional improvement through microinjection, the levels of intracellular ATP in individual oocytes of the three groups were determined ATP levels in 101 hamster oocytes (41 controls, 29 shams, and 31 microinjected) were measured As shown in Figure 13, the control oocytes contained 526 2 ±289 2 fmoles ATP molecules, the sham oocytes contained an average of 557 2 ± 242 9 fmoles ATP molecules and the microinjected oocytes contained an average of 729 3 ±365 9 fmoles ATP molecules (Fig 13)

Therefore, mitochondrial microinjection improved ATP level of oocytes from old hamsters by 38 6% compared with control group (p=0 006) and by 30 9% compared with sham group (p=0 03), while there is no significant improvement by sham injection One-way ANOVA was used for statistical analysis

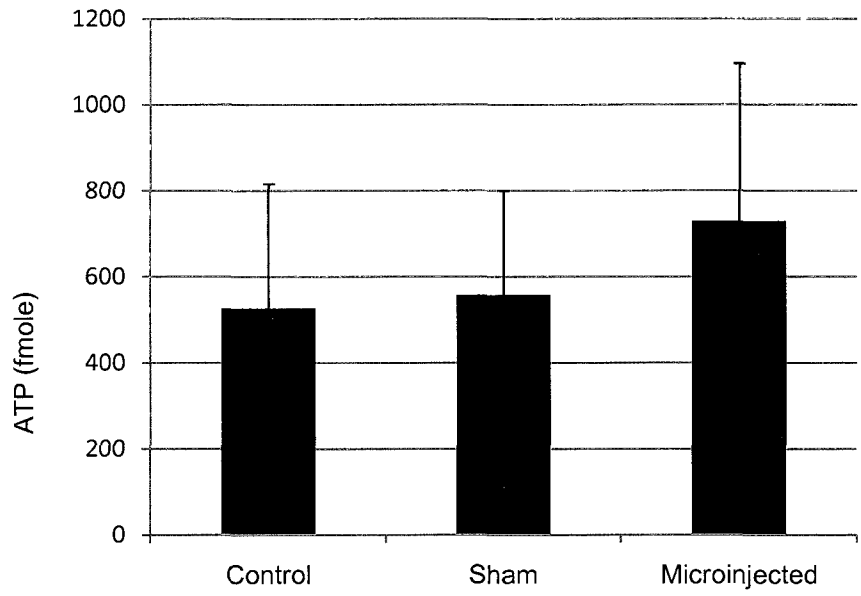

FIG.13. Quantification of ATP in oocytes from control, sham and microinjected groups. Hamster oocytes (101) were measured for ATP level (n=41 of control, 29 of sham, and 31 of microinjected). The control oocytes contained 526.2 ±289.2 fmoles(fM) ATP molecules, sham oocytes an average of 557.2 ± 242.9 fM ATP and microinjected oocytes an average of 729.3 ±365.9 fM ATP. Therefore, mitochondrial microinjection improved ATP level of oocytes from old hamsters by 38.6% compared with control group ($p=0.006$) and by 30.9% compared with sham group ($p=0.03$). No significant improvement took place in the sham injection compared with control ($p=0.684$). The experiments represented 7 old female hamsters. The data are presented as mean ±SD.

Quantification of mitochondria in oocytes from control, sham and microinjected groups-mitochondria labeled with MitoTracker Green FM

Comparisons among fluorescence intensities of oocytes from control, sham and microinjected groups are presented in Figure 14. Cytoplasmic fluorescence intensities of MGF-stained images were analyzed with MetaMorph 7.5. Figure 14 shows a significant increase in the microinjected group compared with control ($p<0.05$) and sham ($p<0.05$) groups. No significant improvement was achieved with sham injection compared to the control group ($p=0.11$). One-way ANOVA was used for statistical analysis.

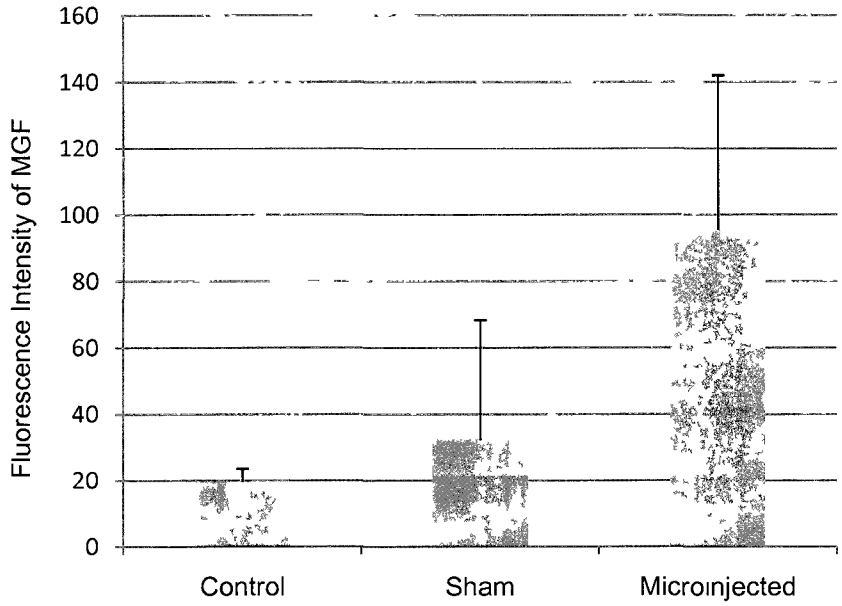

FIG.14. Fluorescent signals in oocytes stained with MitoTracker Green FM. The microinjected group had a significant increase in ooplasmic fluorescence intensity compared with control ($p<0.05$) and sham ($p<0.05$) groups. No significant improvement was achieved with sham injection compared to the control group ($p=0.11$). The experiments represent 30 oocytes in each group from 9 old female golden hamsters. The data are presented as mean ±SD.

Counting mitochondria in pellet with real-time PCR and TEM

The result of real-time PCR showed that there were 40-200 $x10^6$ mitochondria in each pellet. Figure 15 shows the way that mitochondrial number was counted by TEM. The volume of pellet (A) is about $18.7x10^6$ μm^3. There are about 11 mitochondrial (B) per 6 μm^3. Therefore, there are about $3.4x10^7$ mitochondria in each pellet, which is close to the result from real-time PCR.

The mitochondrial pellet was suspended in 20 µl medium and only 10-15 pl mitochondrial suspension was injected into one oocyte, therefore only about 17-100 mitochondria were injected into each oocyte.

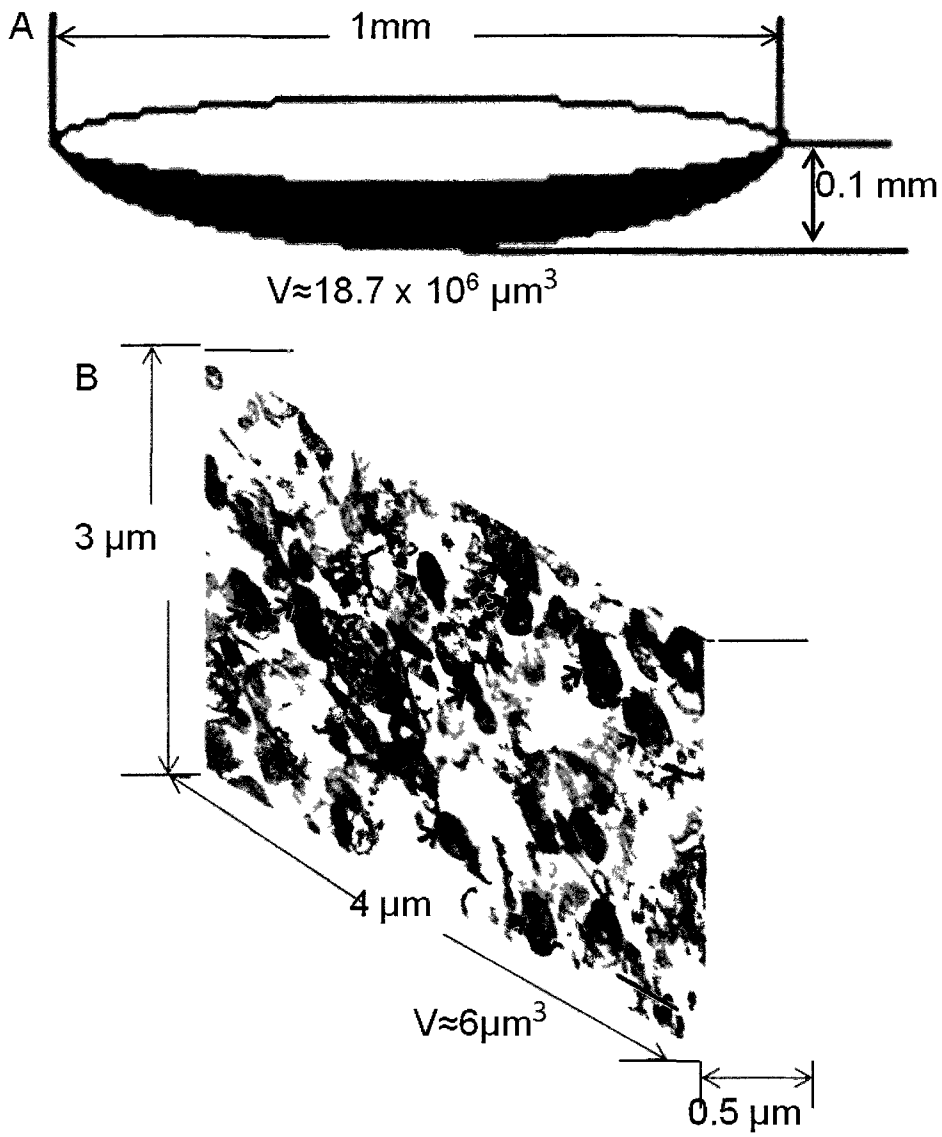

FIG 15 Counting mitochondria in pellet with TEM **A)** The volume of pellet is about 18 7x106 μm^3 **B)** There are about 11 mitochondrial per 6 μm^3 Therefore, there are about 3 4x10^7 mitochondria in each pellet (Bar=500nm)

DISCUSSION

ATP production, apoptosis, calcium regulation and many other important events related to mitochondrial activity are crucial for successful embryo development Van Blerkom has reported increased ATP content in injected M II oocytes of mouse after homologous mitochondrial transfer

[157]. In our study, ATP levels also increased after autologous platelet mitochondrial microinjection. Successful fertilization for human M II oocytes may require a net ATP content of about 2 pmol per oocyte [158, 159], which suggested an ATP content around 2 pmol may be an important threshold for oocyte competence and fertilization. The threshold of ATP content in hamster oocytes for successful fertilization is not clear, but the lower average ATP level in old oocytes reported in our study contributes to the low fertilization of old oocytes. After microinjection with mitochondria, the ATP level of old oocytes even exceeded the ATP level of oocytes from young hamsters as mentioned in chapter II, which may help old oocytes pass the threshold of oocyte competence and embryo development.

However, mitochondrial microinjection did not alleviate the defect of the low mitochondrial numbers in old oocytes. Perez et al. reported in a short note that 5000 mitochondria were injected into mouse oocytes by their group, and Kong et al. reported 3000 mitochondria transferred into a human oocyte [110, 160], but they did not report quantifying the injected number of mitochondria experimentally and estimated from the starting number of cells. For the first time, we measured mitochondrial quantity of recipient oocytes 1 hour after microinjection. In this study, 10-15 pl culture medium with less than 100 isolated platelet mitochondria (determined by TEM and real-time PCR of mitochondrial pellets) were injected into each oocyte in the microinjected group. The small number of injected mitochondria did not change the mitochondrial cohort numbers in oocytes significantly enough to be detected by real-time PCR compared with 50,000 endogenous mitochondria. In addition, one hour of culture is not long enough for significant mtDNA replication. The significant increase in ATP levels suggested that mitochondrial function was improved, even though the transferred mitochondrial number in this study is far less than other reports. Normally, mtDNA copy number remains unchanged until after the blastocyst stage. An early study on the rabbit embryo suggested that the reduced mitochondrial quantity per cell during the pre-implantation stage is apparently accommodated by increased concentrations of ATP generation per mitochondrion [161]. Thus, the microinjection of autologous mitochondria mainly contributed to increased metabolism of mitochondria in the oocytes by improving ATP production and the

failure to increase mitochondrial number by a large amount may not be a necessary factor for improving the fertility rate.

The data from MitoTracker Green FM staining is not consistent with the mtDNA results. The fluorescence intensity of the microinjected group is significantly higher than the sham and control groups. This increase may be due to the following reasons: (1) the oocytes were evaluated about 2 hours after microinjection and the stimulated replication within that time frame may have led to a small increase in mitochondrial number. To confirm this, culturing injected oocytes for a longer time and measuring mtDNA copy number is a future plan. (2) Mitochondrial pellets contained many mitochondrial fragments after the final centrifugation. Since the MitoTracker Green may covalently bind to mitochondrial proteins by reacting with free thiol groups of cysteine residues [128], the large amount of mitochondrial fragments with thiol groups of cysteine residues may have contributed a major part of the increased fluorescence intensity. (3) Microinjection may have led to decreased MMP in a small but significant number of mitochondria, even though the total ATP production was improved by the majority of mitochondria. According to Burckman et al. [139], MitoTracker Green fluorescence intensity was both MMP and oxidation sensitive and fluorescence increased with decreased MMP. The first and third reason can also explain the increase of the fluorescence intensity in the sham group. In the sham group, oocytes may have been stimulated by the insertion of the pipette.

Another phenomenon was found in this study. In oocytes from old hamsters, the ATP level in the control group in Chapter IV was significantly higher ($p=3 \times 10^{-11}$) than those oocytes in Chapter II (Fig. 8A). This difference might have occurred because in Chapter II, we collected oocytes immediately after stripping their cumulus cells. The enzyme treatment would stress the oocytes and the ATP level might have decreased because of this stress. In Chapter IV, we cultured the oocyte for 1 hour after enzyme treatment before collecting them, which allowed the oocytes to recover from stress. The mtDNA copy number in old oocytes in Chapter IV is not higher than that in chapter II (Fig. 8B) significantly ($p=0.14$) (Fig.16). One-way ANOVA was used for statistical analysis.

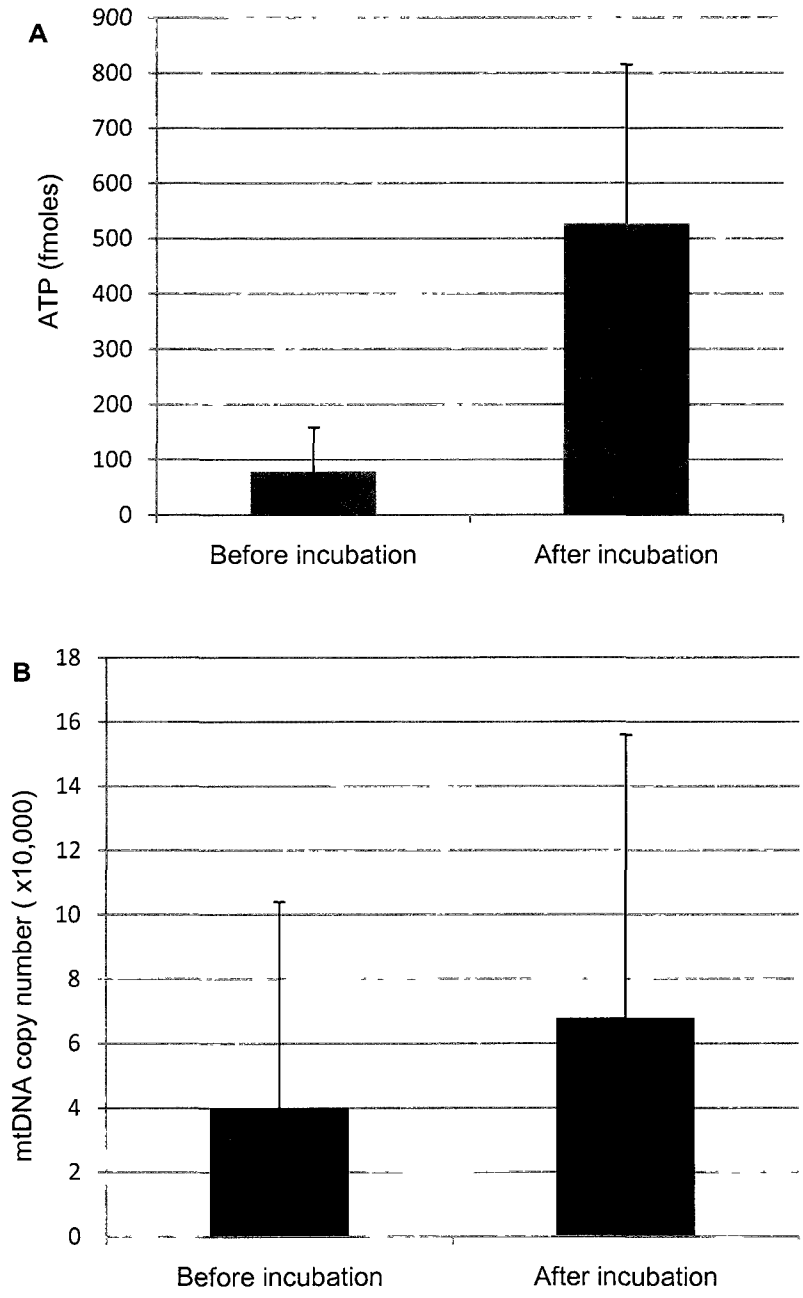

FIG.16. ATP level and mtDNA copy number of oocytes before and after incubation for one hour. **A)** The ATP level in oocytes after incubation is significantly higher ($p=0.03 \times 10^{-9}$, n=55 in "before incubation group", n=29 in "after incubation group") than before. **B)** The mtDNA copy number after incubation is not significantly higher than before incubation (p=0.14, n=55 in "before incubation group", n=29 in "after incubation group").

CHAPTER V

CHANGES IN OOCYTE PRE-IMPLANTATION FERTILIZATION FOLLOWING AUTOLOGOUS PLATELET MITOCHONDRIAL MICROINJECTION

INTRODUCTION

In this study, we planned to determine whether mitochondrial microinjection affects pre-implantation embryo development by comparing the percentage of blastocyst formation among control, sham and microinjected groups.

MATERIALS AND METHODS

Collection of Sperm

Two to six month old male hamsters were administered 0.1-0.2 ml sodium pentobarbital (60 mg/ml) by IP and euthanized via peumothorax and cervical dislocation. A midline incision through the scrotum was carried out to expose testes and locate the vas deferens for excision followed by transfer into M2 medium for sperm collection at 37°C.

In vitro fertilization

Oocytes were collected as previously described and microinjected with autologous mitochondria isolated from platelets. The microinjected oocytes were transferred into M199TE medium and incubated at 37°C, 5% CO_2, 100% H_2O for one hour prior to IVF. A 30 µl sperm droplet was then added to control and microinjected oocytes and incubated at 37°C, 5% CO_2, 100% H_2O for 3 hrs. The fertilized oocytes were transferred into M199TE medium and placed in the incubator at 37°C, 5% CO_2, 100% H_2O for 24 hrs followed by transfer into hamster embryo culture medium 9 (HECM-9) [162] (Table 3) for blastocyst evaluation 72 hrs later.

Evaluation of blastocyst development

The cultured fertilized oocytes were evaluated for blastocyst embryo development at 72 and 96 hours by light microscopy.

RESULTS

In vitro fertilization

A total of 312 hamster oocytes were fertilized with sperm (control N=132, sham N=89 and microinjection N=91). The IVF rate was determined by the percentage of fertilized embryos

developing to the blastocyst stage. The sham group demonstrated a higher percentage of blastocyst embryo development (69%) than control (58%) and microinjected (55%) groups (Fig.17). χ^2 test was used for statistical analysis.

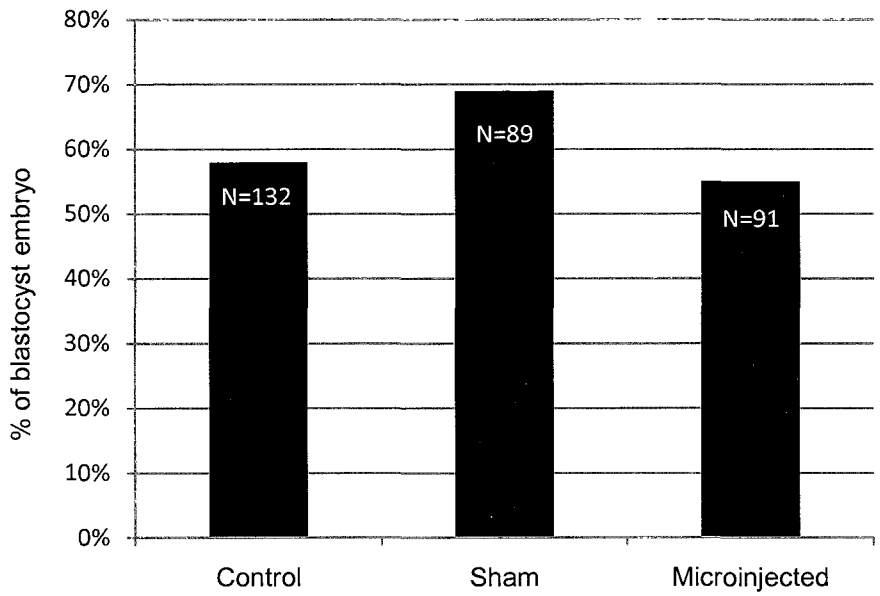

FIG. 17. *In vitro* fertility rate of pre-implantation embryos. The IVF rate (determined by percent blastocyst embryo development) of mature oocytes of sham group (69%) was higher than control (58%) and microinjected (55%) groups. The experiments represented 22 old female golden hamsters. There are no significant differences among three groups($p>0.05$).

DISCUSSION

According to the data in Figure 17, autologous mitochondria microinjection did not seem to significantly enhance blastocyst development. Though the sham group illustrates a higher percentage of blastocyst embryos than control and microinjection groups there is no significant difference. Previous reports have indicated improvement in oocyte quality and fertilization using mitochondria isolated from granulosa cells [111, 163]. However, Takeda et al. [164] showed that exogenous mitochondria delay parthenogenic development of murine oocytes. Autologous

platelet mitochondria microinjection into oocytes enhanced ATP production but did not improve blastocyst formation. One reason for such observations could be that injected mitochondria affect embryo development during late pre-implantation and post-implantation stages, but not during the cleavage stage [111]. One study showed that mitochondria are morphologically undifferentiated and generate relatively low levels of ATP in mature M II mammalian oocytes and early cleavage embryos in comparison to blastocyst embryos [111]. Generally, the mtDNA copy number does not change until the blastocyst stage [165]. The unchanged mitochondrial quantity of microinjected oocytes may not influence the embryo cleavage, and the effect of increased ATP levels within the oocyte may improve the fertility rate during post-implantation stages. Therefore the fact that we saw no significant increase in blastocyst formation does not mean that autologous platelet mitochondrial microinjection cannot improve the fertility rate. Measurement of post-implantation conditions should be performed to see the final effect of this method.

CHAPTER VI

CONCLUSION

Numerous age-related morphological and functional mitochondrial changes have been demonstrated in oocytes from old and young Syrian hamsters. They include increase of electron density, complexity of mitochondrial ultrastructure and ROS level, decrease of mitochondrial quantity, decrease of MMP and ATP production. Morphological changes of oocytes determined by the perivitelline space showed that young hamsters ovulated more "healthy looking" oocytes than old hamsters.

Platelets can be a good source for mitochondrial transfer since no differences in ATP production and morphology were seen between old and young hamsters. Lower common mtDNA mutation frequency and anucleate are other two advantages of platelets as a source for mitochondrial transfer.

Autologous platelet mitochondrial microinjection could improve ATP production of recipient oocytes without significantly changing mitochondrial quantity, although we saw no impact on pre-implantation fertility rate as determined by the percentage of blastocyst development. However further studies examining the post implantation fertility rate may reveal a positive influence of mitochondrial microinjection on aging oocytes.

REFERENCES

1. Tam PP, Zhou SX. The allocation of epiblast cells to ectodermal and germ-line lineages is influenced by the position of the cells in the gastrulating mouse embryo. Dev Biol 1996; 178:124-132.

2. Parkening TA, Collins TJ, Lau IF, Saksena SK. The pituitary-ovarian complex in the aged anoestrous golden hamster. J Reprod Fertil 1982; 64:37-46.

3. Gondos B, Westergaard L, Byskov AG. Initiation of oogenesis in the human fetal ovary: ultrastructural and squash preparation study. Am J Obstet Gynecol 1986; 155:189-195.

4. Byskov AG, Hoyer PE, Westergaard L. Origin and differentiation of the endocrine cells of the ovary. J Reprod Fertil 1985; 75:299-306.

5. Yu N, Roy SK. Development of primordial and prenatal follicles from undifferentiated somatic cells and oocytes in the hamster prenatal ovary in vitro: effect of insulin. Biol Reprod 1999; 61:1558-1567.

6. Eppig JJ, O'Brien MJ. Development in vitro of mouse oocytes from primordial follicles. Biol Reprod 1996; 54:197-207.

7. Weakley BS. Light and electron microscopy of developing germ cells and follicle cells in the ovary of the golden hamster: twenty-four hours before birth to eight days post partum. J Anat 1967; 101:435-459.

8. Channing CP, Schaerf FW, Anderson LD, Tsafriri A. Ovarian follicular and luteal physiology. Int Rev Physiol 1980; 22:117-201.

9. Trounson A, Anderiesz C, Jones GM, Kausche A, Lolatgis N, Wood C. Oocyte maturation. Hum Reprod 1998; 13 Suppl 3:52-62; discussion 71-55.

10. de Bruin JP, Dorland M, Spek ER, Posthuma G, van Haaften M, Looman CW, te Velde ER. Age-related changes in the ultrastructure of the resting follicle pool in human ovaries. Biol Reprod 2004; 70:419-424.

11. Yap C. Ontogeny: the evolution of an oocyte. Obstet Gynecol Surv 2000; 55:449-454.

12. Al-Sunaidi M, Al-Mahrizi S, Tan SL, Tulandi T. Age-related changes in antral follicle count among women with and without polycystic ovaries. Gynecol Obstet Invest 2007; 64:199-203.

13. Spira A. The decline of fecundity with age. Maturitas 1988; Suppl 1:15-22.

14. te Velde ER, Pearson PL. The variability of female reproductive ageing. Hum Reprod Update 2002; 8:141-154.

15. van Noord-Zaadstra BM, Looman CW, Alsbach H, Habbema JD, te Velde ER, Karbaat J. *Delaying childbearing: effect of age on fecundity and outcome of pregnancy.* BMJ 1991; 302:1361-1365.

16. Tosti E, Boni, R. Oocyte maturation and fertilization: A long history for a short event. Bentham: Bentham Science Publishers; 2011.

17. http://www.americanpregnancy.org/infertility/ivf.html.

18. Broekmans FJ, Soules MR, Fauser BC. Ovarian aging: mechanisms and clinical consequences. Endocr Rev 2009; 30:465-493.

19. Alberts B, Johnson A, Lewis J, Raff M, Roberts K, walter P. Molecular biology of the cell. New York: Garland Science; 2002.

20. Perkins G, Renken C, Martone ME, Young SJ, Ellisman M, Frey T. Electron tomography of neuronal mitochondria: three-dimensional structure and organization of cristae and membrane contacts. J Struct Biol 1997; 119:260-272.

21. Scheffler IE. Mitochondria. Hoboken, N.J.: Wiley-Liss; 2008.

22. Mannella CA. Structure and dynamics of the mitochondrial inner membrane cristae. Biochim Biophys Acta 2006; 1763:542-548.

23. Reed JC, Green DR. Apoptosis : physiology and pathology. Cambridge: Cambridge University Press; 2011.

24. Green DR, Reed JC. Mitochondria and apoptosis. Science 1998; 281:1309-1312.
25. Susin SA, Zamzami N, Kroemer G. Mitochondria as regulators of apoptosis: doubt no more. Biochim Biophys Acta 1998; 1366:151-165.

26. Brand FN, Kiely DK, Kannel WB, Myers RH. Family patterns of coronary heart disease mortality: the Framingham Longevity Study. J Clin Epidemiol 1992; 45:169-174.

27. De Benedictis G, Rose G, Carrieri G, De Luca M, Falcone E, Passarino G, Bonafe M, Monti D, Baggio G, Bertolini S, Mari D, Mattace R, et al. Mitochondrial DNA inherited variants are associated with successful aging and longevity in humans. FASEB J 1999; 13:1532-1536.

28. Harman D. Aging: a theory based on free radical and radiation chemistry. J Gerontol 1956; 11:298-300.

29. Harman D. The biologic clock: the mitochondria? J Am Geriatr Soc 1972; 20:145-147.

30. Loeb LA, Wallace DC, Martin GM. The mitochondrial theory of aging and its relationship to reactive oxygen species damage and somatic mtDNA mutations. Proc Natl Acad Sci U S A 2005; 102:18769-18770.

31. Prolla TA, Bohr VA, de Souza-Pinto NC. Mitochondria and aging. Mech Ageing Dev 2010; 131:449-450.

32. Kujoth GC, Hiona A, Pugh TD, Someya S, Panzer K, Wohlgemuth SE, Hofer T, Seo AY, Sullivan R, Jobling WA, Morrow JD, Van Remmen H, et al. Mitochondrial DNA mutations, oxidative stress, and apoptosis in mammalian aging. Science 2005; 309:481-484.

33. Trifunovic A, Hansson A, Wredenberg A, Rovio AT, Dufour E, Khvorostov I, Spelbrink JN, Wibom R, Jacobs HT, Larsson NG. Somatic mtDNA mutations cause aging phenotypes without affecting reactive oxygen species production. Proc Natl Acad Sci U S A 2005; 102:17993-17998.

34. Alexeyev MF, Ledoux SP, Wilson GL. Mitochondrial DNA and aging. Clin Sci (Lond) 2004; 107:355-364.

35. Wunderlich V, Schutt M, Bottger M, Graffi A. Preferential alkylation of mitochondrial deoxyribonucleic acid by N-methyl-N-nitrosourea. Biochem J 1970; 118:99-109.

36. Backer JM, Weinstein IB. Mitochondrial DNA is a major cellular target for a dihydrodiol-epoxide derivative of benzo[a]pyrene. Science 1980; 209:297-299.

37. Rossi SC, Gorman N, Wetterhahn KE. Mitochondrial reduction of the carcinogen chromate: formation of chromium(V). Chem Res Toxicol 1988; 1:101-107.

38. Boveris A, Oshino N, Chance B. The cellular production of hydrogen peroxide. Biochem J 1972; 128:617-630.

39. Loschen G, Azzi A, Richter C, Flohe L. Superoxide radicals as precursors of mitochondrial hydrogen peroxide. FEBS Lett 1974; 42:68-72.

40. Cadenas E, Boveris A, Ragan CI, Stoppani AO. Production of superoxide radicals and hydrogen peroxide by NADH-ubiquinone reductase and ubiquinol-cytochrome c reductase from beef-heart mitochondria. Arch Biochem Biophys 1977; 180:248-257.

41. Turrens JF, Alexandre A, Lehninger AL. Ubisemiquinone is the electron donor for superoxide formation by complex III of heart mitochondria. Arch Biochem Biophys 1985; 237:408-414.

42. Liu Y, Fiskum G, Schubert D. Generation of reactive oxygen species by the mitochondrial electron transport chain. J Neurochem 2002; 80:780-787.

43. Murphy MP, Brand MD. Variable stoichiometry of proton pumping by the mitochondrial respiratory chain. Nature 1987; 329:170-172.

44. Chen LB. Mitochondrial membrane potential in living cells. Annu Rev Cell Biol 1988; 4:155-181.

45. Reid RA, Moyle J, Mitchell P. Synthesis of adenosine triphosphate by a protonmotive force in rat liver mitochondria. Nature 1966; 212:257-258.

46. Azzone GF, Pozzan T, Viola E, Arslan P. Proton electrochemical gradient and phosphate potential in submitochondrial particles. Biochim Biophys Acta 1978; 501:317-329.

47. LaNoue KF, Schoolwerth AC. Metabolite transport in mitochondria. Annu Rev Biochem 1979; 48:871-922.

48. Chen WJ, Douglas MG. The role of protein structure in the mitochondrial import pathway. Unfolding of mitochondrially bound precursors is required for membrane translocation. J Biol Chem 1987; 262:15605-15609.

49. Eilers M, Verner K, Hwang S, Schatz G. Import of proteins into mitochondria. Philos Trans R Soc Lond B Biol Sci 1988; 319:121-126.

50. Martin NC, Rabinowitz M, Fukuhara H. Yeast mitochondrial DNA specifies tRNA for 19 amino acids. Deletion mapping of the tRNA genes. Biochemistry 1977; 16:4672-4677.

51. Abou-Khalil WH, Arimura GK, Yunis AA, Abou-Khalil S. Inhibition by rhodamine 123 of protein synthesis in mitochondria of normal and cancer tissues. Biochem Biophys Res Commun 1986; 137:759-765.

52. Darzynkiewicz Z, Staiano-Coico L, Melamed MR. Increased mitochondrial uptake of rhodamine 123 during lymphocyte stimulation. Proc Natl Acad Sci U S A 1981; 78:2383-2387.

53. Levenson R, Macara IG, Smith RL, Cantley L, Housman D. Role of mitochondrial membrane potential in the regulation of murine erythroleukemia cell differentiation. Cell 1982; 28:855-863.

54. Heath-Engel HM, Shore GC. Mitochondrial membrane dynamics, cristae remodelling and apoptosis. Biochim Biophys Acta 2006; 1763:549-560.

55. Malka F, Guillery O, Cifuentes-Diaz C, Guillou E, Belenguer P, Lombes A, Rojo M. Separate fusion of outer and inner mitochondrial membranes. EMBO Rep 2005; 6:853-859.

56. Kroemer G, Petit P, Zamzami N, Vayssiere JL, Mignotte B. The biochemistry of programmed cell death. FASEB J 1995; 9:1277-1287.

57. Halestrap AP. What is the mitochondrial permeability transition pore? J Mol Cell Cardiol 2009; 46:821-831.

58. Haworth RA, Hunter DR. The Ca2+-induced membrane transition in mitochondria. II. Nature of the Ca2+ trigger site. Arch Biochem Biophys 1979; 195:460-467.

59. Vyssokikh MY, Brdiczka D. The function of complexes between the outer mitochondrial membrane pore (VDAC) and the adenine nucleotide translocase in regulation of energy metabolism and apoptosis. Acta Biochim Pol 2003; 50:389-404.

60. Crompton M. The mitochondrial permeability transition pore and its role in cell death. Biochem J 1999; 341 (Pt 2):233-249.

61. Toninello A, Salvi M, Mondovi B. Interaction of biologically active amines with mitochondria and their role in the mitochondrial-mediated pathway of apoptosis. Curr Med Chem 2004; 11:2349-2374.

62. Kinnally KW, Antonsson B. A tale of two mitochondrial channels, MAC and PTP, in apoptosis. Apoptosis 2007; 12:857-868.

63. Wallace DC. The mitochondrial genome in human adaptive radiation and disease: on the road to therapeutics and performance enhancement. Gene 2005; 354:169-180.

64. Bootman MD, Collins TJ, Peppiatt CM, Prothero LS, MacKenzie L, De Smet P, Travers M, Tovey SC, Seo JT, Berridge MJ, Ciccolini F, Lipp P. Calcium signalling - an overview. Semin Cell Dev Biol 2001; 12:3-10.

65. Grijalba MT, Vercesi AE, Schreier S. Ca2+-induced increased lipid packing and domain formation in submitochondrial particles. A possible early step in the mechanism of Ca2+-stimulated generation of reactive oxygen species by the respiratory chain. Biochemistry 1999; 38:13279-13287.

66. Ott M, Gogvadze V, Orrenius S, Zhivotovsky B. Mitochondria, oxidative stress and cell death. Apoptosis 2007; 12:913-922.

67. Ishida A, Mashima H, Tanaka S. Intracellular distribution of calcium in cardiac muscles studied by electron microscope autoradiography. Jpn J Physiol 1979; 29:37-48.

68. Burger G, Lang BF. Parallels in genome evolution in mitochondria and bacterial symbionts. IUBMB Life 2003; 55:205-212.

69. Fernandez-Silva P, Enriquez JA, Montoya J. Replication and transcription of mammalian mitochondrial DNA. Exp Physiol 2003; 88:41-56.

70. Richter C, Park JW, Ames BN. Normal oxidative damage to mitochondrial and nuclear DNA is extensive. Proc Natl Acad Sci U S A 1988; 85:6465-6467.

71. Chung SS, Eimon PM, Weindruch R, Aiken JM. Analysis of age-associated mitochondrial DNA deletion breakpoint regions from mice suggests a novel model of deletion formation. Age 1996; 19:117-128.

72. Wang LY, Wang DH, Zou XY, Xu CM. Mitochondrial functions on oocytes and preimplantation embryos. J Zhejiang Univ Sci B 2009; 10:483-492.

73. Eppig JJ. Coordination of nuclear and cytoplasmic oocyte maturation in eutherian mammals. Reprod Fertil Dev 1996; 8:485-489.

74. Torner H, Brussow KP, Alm H, Ratky J, Pohland R, Tuchscherer A, Kanitz W. Mitochondrial aggregation patterns and activity in porcine oocytes and apoptosis in surrounding cumulus cells depends on the stage of pre-ovulatory maturation. Theriogenology 2004; 61:1675-1689.

75. Jansen RP, de Boer K. The bottleneck: mitochondrial imperatives in oogenesis and ovarian follicular fate. Mol Cell Endocrinol 1998; 145:81-88.

76. Sathananthan AH. Ultrastructure of the human egg. Hum Cell 1997; 10:21-38.

77. Kuwahara H, Horie T, Ishikawa S, Tsuda C, Kawakami S, Noda Y, Kaneko T, Tahara S, Tachibana T, Okabe M, Melki J, Takano R, et al. Oxidative stress in skeletal muscle causes severe disturbance of exercise activity without muscle atrophy. Free Radic Biol Med 2010; 48:1252-1262.

78. Zeng HT, Yeung WS, Cheung MP, Ho PC, Lee CK, Zhuang GL, Liang XY, O WS. In vitro-matured rat oocytes have low mitochondrial deoxyribonucleic acid and adenosine triphosphate contents and have abnormal mitochondrial redistribution. Fertil Steril 2009; 91:900-907.

79. Ottolenghi C, Uda M, Hamatani T, Crisponi L, Garcia JE, Ko M, Pilia G, Sforza C, Schlessinger D, Forabosco A. Aging of oocyte, ovary, and human reproduction. Ann N Y Acad Sci 2004; 1034:117-131.

80. Sharov AA, Falco G, Piao Y, Poosala S, Becker KG, Zonderman AB, Longo DL, Schlessinger D, Ko M. Effects of aging and calorie restriction on the global gene expression profiles of mouse testis and ovary. BMC Biol 2008; 6:24.

81. Jansen RP, Burton GJ. Mitochondrial dysfunction in reproduction. Mitochondrion 2004; 4:577-600.

82. Wilding M, Dale B, Marino M, di Matteo L, Alviggi C, Pisaturo ML, Lombardi L, De Placido G. Mitochondrial aggregation patterns and activity in human oocytes and preimplantation embryos. Hum Reprod 2001; 16:909-917.

83. Fan W, Kou H, Shen D, LeRoy EC. Identification of altered expression of ADP/ATP translocase during cellular senescence in vitro. Exp Gerontol 1998; 33:457-465.

84. Van Blerkom J, Davis P, Alexander S. Inner mitochondrial membrane potential (DeltaPsim), cytoplasmic ATP content and free Ca2+ levels in metaphase II mouse oocytes. Hum Reprod 2003; 18:2429-2440.

85. Van Blerkom J, Davis P. Mitochondrial signaling and fertilization. Mol Hum Reprod 2007; 13:759-770.

86. Thouas GA, Trounson AO, Wolvetang EJ, Jones GM. Mitochondrial dysfunction in mouse oocytes results in preimplantation embryo arrest in vitro. Biol Reprod 2004; 71:1936-1942.

87 Van Blerkom J, Cox H, Davis P Regulatory roles for mitochondria in the peri-implantation mouse blastocyst possible origins and developmental significance of differential DeltaPsim Reproduction 2006, 131 961-976

88 Van Blerkom J, Runner MN Mitochondrial reorganization during resumption of arrested meiosis in the mouse oocyte Am J Anat 1984, 171 335-355

89 Dumollard R, Hammar K, Porterfield M, Smith PJ, Cibert C, Rouviere C, Sardet C Mitochondrial respiration and Ca2+ waves are linked during fertilization and meiosis completion Development 2003, 130 683-692

90 Perez GI, Trbovich AM, Gosden RG, Tilly JL Mitochondria and the death of oocytes Nature 2000, 403 500-501

91 Krakauer DC, Mira A Mitochondria and germ-cell death Nature 1999, 400 125-126

92 Wu J, Zhang L, Wang X Maturation and apoptosis of human oocytes in vitro are age-related Fertil Steril 2000, 74 1137-1141

93 Cassara MC, Menzel VA, Hinsch KD, Wrenzycki C, Hinsch E Voltage-dependent anion channels 1 and 2 are expressed in porcine oocytes Biosci Rep 2010, 30 193-200

94 Spikings EC, Alderson J, St John JC Regulated mitochondrial DNA replication during oocyte maturation is essential for successful porcine embryonic development Biol Reprod 2007, 76 327-335

95 Lopez-Lluch G, Irusta PM, Navas P, de Cabo R Mitochondrial biogenesis and healthy aging Exp Gerontol 2008, 43 813-819

96 Munne S, Sultan KM, Weier HU, Grifo JA, Cohen J, Rosenwaks Z Assessment of numeric abnormalities of X, Y, 18, and 16 chromosomes in preimplantation human embryos before transfer Am J Obstet Gynecol 1995, 172 1191-1199, discussion 1199-1201

97 Yin H, Baart E, Betzendahl I, Eichenlaub-Ritter U Diazepam induces meiotic delay, aneuploidy and predivision of homologues and chromatids in mammalian oocytes Mutagenesis 1998, 13 567-580

98 Golsteyn RM, Schultz SJ, Bartek J, Ziemiecki A, Ried T, Nigg EA Cell cycle analysis and chromosomal localization of human Plk1, a putative homologue of the mitotic kinases Drosophila polo and Saccharomyces cerevisiae Cdc5 J Cell Sci 1994, 107 (Pt 6) 1509-1517

99 Zhang X, Wu XQ, Lu S, Guo YL, Ma X Deficit of mitochondria-derived ATP during oxidative stress impairs mouse MII oocyte spindles Cell Res 2006, 16 841-850

100 Tarin JJ Potential effects of age-associated oxidative stress on mammalian oocytes/embryos Mol Hum Reprod 1996, 2 717-724

101 Eichenlaub-Ritter U Genetics of oocyte ageing Maturitas 1998, 30 143-169

102 Van Blerkom J Microtubule mediation of cytoplasmic and nuclear maturation during the early stages of resumed meiosis in cultured mouse oocytes Proc Natl Acad Sci U S A 1991, 88 5031-5035

103 Nagai S, Mabuchi T, Hirata S, Shoda T, Kasai T, Yokota S, Shitara H, Yonekawa H, Hoshi K Correlation of abnormal mitochondrial distribution in mouse oocytes with reduced developmental competence Tohoku J Exp Med 2006, 210 137-144

104 Krisher RL The effect of oocyte quality on development J Anim Sci 2004, 82 E-Suppl E14-23

105 Miao YL, Kikuchi K, Sun QY, Schatten H Oocyte aging cellular and molecular changes, developmental potential and reversal possibility Hum Reprod Update 2009, 15 573-585

106 Bos-Mikich A, Swann K, Whittingham DG Calcium oscillations and protein synthesis inhibition synergistically activate mouse oocytes Mol Reprod Dev 1995, 41 84-90

107 Kurokawa M, Sato K, Fissore RA Mammalian fertilization from sperm factor to phospholipase Czeta Biol Cell 2004, 96 37-45

108 Yoon SY, Fissore RA Release of phospholipase C zetaand [Ca2+]i oscillation-inducing activity during mammalian fertilization Reproduction 2007, 134 695-704

109 Whitaker M Calcium signalling in early embryos Philos Trans R Soc Lond B Biol Sci 2008, 363 1401-1418

110 Kong LH, Liu Z, Li H, Zhu L, Chen SM, Chen SL, Xing FQ [Mitochondria transfer from self-granular cells to improve embryos' quality] Zhonghua Fu Chan Ke Za Zhi 2004, 39 105-107

111 Hua S, Zhang Y, Li XC, Ma LB, Cao JW, Dai JP, Li R Effects of granulosa cell mitochondria transfer on the early development of bovine embryos in vitro Cloning Stem Cells 2007, 9 237-246

112 Seifer DB, DeJesus V, Hubbard K Mitochondrial deletions in luteinized granulosa cells as a function of age in women undergoing in vitro fertilization Fertil Steril 2002, 78 1046-1048

113 Tsai HD, Hsieh YY, Hsieh JN, Chang CC, Yang CY, Yang JG, Cheng WL, Tsai FJ, Liu CS Mitochondria DNA deletion and copy numbers of cumulus cells associated with in vitro fertilization outcomes J Reprod Med 2010, 55 491-497

114 Herbert RA Human Anatomy and Physiology - Marieb,En International Journal of Nursing Studies 1990, 27 97-98

115 Mohamed SA, Wesch D, Blumenthal A, Bruse P, Windler K, Ernst M, Kabelitz D, Oehmichen M, Meissner C Detection of the 4977 bp deletion of mitochondrial DNA in different human blood cells Exp Gerontol 2004, 39 181-188

116 Bex FJ, Goldman BD Serum gonadotropins associated with puberty in the female Syrian hamster Biol Reprod 1977, 16 557-560

117 Kent GC, Ridgway PM, Strobel EF Continual light and constant estrus in hamsters Endocrinology 1968, 82 699-703

118 Darrow JM, Davis FC, Elliott JA, Stetson MH, Turek FW, Menaker M Influence of photoperiod on reproductive development in the golden hamster Biol Reprod 1980, 22 443-450

119 Thomas CM, Bastiaans LA, Rolland R Ovulation, ovum transport and implantation in the adult golden hamster Eur J Obstet Gynecol Reprod Biol 1981, 12 257-265

120. Greenwald GS. Analysis of superovulation in the adult hamster. Endocrinology 1962; 71:378-389.

121. Ridley K, Greenwald GS. Progesterone levels measured every two hours in the cyclic hamster. Proc Soc Exp Biol Med 1975; 149:10-12.

122. Yamauchi Y, Yanagimachi R, Horiuchi T. Full-term development of golden hamster oocytes following intracytoplasmic sperm head injection. Biol Reprod 2002; 67:534-539.

123. Mizoguchi H, Dukelow WR. Fertilizability of ova from young or old hamsters after spontaneous or induced ovulation. Fertil Steril 1981; 35:79-83.

124. Yanagimachi R, Chang MC. In Vitro Fertilization of Golden Hamster Ova. J Exp Zool 1964; 156:361-375.

125. Xia P. Intracytoplasmic sperm injection: correlation of oocyte grade based on polar body, perivitelline space and cytoplasmic inclusions with fertilization rate and embryo quality. Hum Reprod 1997; 12:1750-1755.

126. Van Blerkom J, Davis P, Mathwig V, Alexander S. Domains of high-polarized and low-polarized mitochondria may occur in mouse and human oocytes and early embryos. Hum Reprod 2002; 17:393-406.

127. Kweon SM, Kim HJ, Lee ZW, Kim SJ, Kim SI, Paik SG, Ha KS. Real-time measurement of intracellular reactive oxygen species using Mito tracker orange (CMH2TMRos). Biosci Rep 2001; 21:341-352.

128. Presley AD, Fuller KM, Arriaga EA. MitoTracker Green labeling of mitochondrial proteins and their subsequent analysis by capillary electrophoresis with laser-induced fluorescence detection. J Chromatogr B Analyt Technol Biomed Life Sci 2003; 793:141-150.

129. Maagaard A, Holberg-Petersen M, Kvittingen EA, Sandvik L, Bruun JN. Depletion of mitochondrial DNA copies/cell in peripheral blood mononuclear cells in HIV-1-infected treatment-naive patients. HIV Med 2006; 7:53-58.

130. Britton AP, Moon YS, Yuen BH. A simple handling technique for mammalian oocytes and embryos during preparation for transmission electron microscopy. J Microsc 1991; 161:497-499.

131. Rienzi L, Ubaldi FM, Iacobelli M, Minasi MG, Romano S, Ferrero S, Sapienza F, Baroni E, Litwicka K, Greco E. Significance of metaphase II human oocyte morphology on ICSI outcome. Fertil Steril 2008; 90:1692-1700.

132. Haugland RP, Spence MTZ, Johnson ID. Handbook of fluorescent probes and research chemicals. Eugene, OR, USA (4849 Pitchford Ave., Eugene 97402): Molecular Probes; 1996.

133. Smith J, Ladi E, Mayer-Proschel M, Noble M. Redox state is a central modulator of the balance between self-renewal and differentiation in a dividing glial precursor cell. Proc Natl Acad Sci U S A 2000; 97:10032-10037.

134. Shoubridge EA, Wai T. Mitochondrial DNA and the mammalian oocyte. Curr Top Dev Biol 2007; 77:87-111.

135. Cavelier L, Johannisson A, Gyllensten U. Analysis of mtDNA copy number and composition of single mitochondrial particles using flow cytometry and PCR. Exp Cell Res 2000; 259:79-85.

136 Weibel ER, Kistler GS, Scherle WF Practical stereological methods for morphometric cytology J Cell Biol 1966, 30 23-38

137 Reynier P, May-Panloup P, Chretien MF, Morgan CJ, Jean M, Savagner F, Barriere P, Malthiery Y Mitochondrial DNA content affects the fertilizability of human oocytes Mol Hum Reprod 2001, 7 425-429

138 Santos TA, El Shourbagy S, St John JC Mitochondrial content reflects oocyte variability and fertilization outcome Fertil Steril 2006, 85 584-591

139 Buckman JF, Hernandez H, Kress GJ, Votyakova TV, Pal S, Reynolds IJ MitoTracker labeling in primary neuronal and astrocytic cultures influence of mitochondrial membrane potential and oxidants J Neurosci Methods 2001, 104 165-176

140 Keij JF, Bell-Prince C, Steinkamp JA Staining of mitochondrial membranes with 10-nonyl acridine orange, MitoFluor Green, and MitoTracker Green is affected by mitochondrial membrane potential altering drugs Cytometry 2000, 39 203-210

141 Brookes PS Mitochondrial H(+) leak and ROS generation an odd couple Free Radic Biol Med 2005, 38 12-23

142 Speakman JR, Talbot DA, Selman C, Snart S, McLaren JS, Redman P, Krol E, Jackson DM, Johnson MS, Brand MD Uncoupled and surviving individual mice with high metabolism have greater mitochondrial uncoupling and live longer Aging Cell 2004, 3 87-95

143 Roy MK, Thalang VN, Trakoontivakorn G, Nakahara K Mechanism of mahanine-induced apoptosis in human leukemia cells (HL-60) Biochem Pharmacol 2004, 67 41-51

144 Weakley BS, James JL Differentiation of endoplasmic reticulum in the developing oocyte of the golden hamster (Mesocricetus auratus) Cell Tissue Res 1982, 223 127-139

145 Banno T, Kohno K Conformational changes of smooth endoplasmic reticulum induced by brief anoxia in rat Purkinje cells J Comp Neurol 1996, 369 462-471

146 Jones HW, Jr , Cooke I, Kempers R, Brinsden P, Saunders D International Federation of Fertility Societies Surveillance 2010 preface Fertil Steril 2011, 95 491

147 J, Scott R, Alikani M, Schimmel T, Munne S, Levron J, Wu L, Brenner C, Warner C, Willadsen S Ooplasmic transfer in mature human oocytes Mol Hum Reprod 1998, 4 269-280

148 Shuster RC, Rubenstein AJ, Wallace DC Mitochondrial DNA in anucleate human blood cells Biochem Biophys Res Commun 1988, 155 1360-1365

149 Jenuth JP, Peterson AC, Shoubridge EA Tissue-specific selection for different mtDNA genotypes in heteroplasmic mice Nat Genet 1997, 16 93-95

150 Suissa S, Wang Z, Poole J, Wittkopp S, Feder J, Shutt TE, Wallace DC, Shadel GS, Mishmar D Ancient mtDNA genetic variants modulate mtDNA transcription and replication PLoS Genet 2009, 5 e1000474

151 Corral-Debrinski M, Horton T, Lott MT, Shoffner JM, Beal MF, Wallace DC Mitochondrial DNA deletions in human brain regional variability and increase with advanced age Nat Genet 1992, 2 324-329

152. GA, Shibata D, Soong NW, Arnheim N. A pattern of accumulation of a somatic deletion of mitochondrial DNA in aging human tissues. Proc Natl Acad Sci U S A 1992; 89:7370-7374.

153. Kao S, Chao HT, Wei YH. Mitochondrial deoxyribonucleic acid 4977-bp deletion is associated with diminished fertility and motility of human sperm. Biol Reprod 1995; 52:729-736.

154. Meissner C, Bruse P, Mohamed SA, Schulz A, Warnk H, Storm T, Oehmichen M. The 4977 bp deletion of mitochondrial DNA in human skeletal muscle, heart and different areas of the brain: a useful biomarker or more? Exp Gerontol 2008; 43:645-652.

155. Shrivastava M, Das TK, Behari M, Pati U, Vivekanandhan S. Ultrastructural variations in platelets and platelet mitochondria: a novel feature in amyotrophic lateral sclerosis. Ultrastruct Pathol 2011; 35:52-59.

156. Graham J, Ford T, Rickwood D. The preparation of subcellular organelles from mouse liver in self-generated gradients of iodixanol. Anal Biochem 1994; 220:367-373.

157. Van Blerkom J, Sinclair J, Davis P. Mitochondrial transfer between oocytes: potential applications of mitochondrial donation and the issue of heteroplasmy. Hum Reprod 1998; 13:2857-2868.

158. Van Blerkom J, Davis PW, Lee J. ATP content of human oocytes and developmental potential and outcome after in-vitro fertilization and embryo transfer. Hum Reprod 1995; 10:415-424.

159. Zeng HT, Ren Z, Yeung WS, Shu YM, Xu YW, Zhuang GL, Liang XY. Low mitochondrial DNA and ATP contents contribute to the absence of birefringent spindle imaged with PolScope in in vitro matured human oocytes. Hum Reprod 2007; 22:1681-1686.

160. Kong LH, Liu Z, Li H, Zhu L, Xing FQ. Pregnancy in a 46-year-old woman after autologous granular cell mitochondria transfer. Di Yi Jun Yi Da Xue Xue Bao 2003; 23:743, 747.

161. Van Blerkom J, Manes C, Daniel JC, Jr. Development of preimplantation rabbit embryos in vivo and in vitro. I. An ultrastructural comparison. Dev Biol 1973; 35:262-282.

162. McKiernan SH, Bavister BD. Culture of one-cell hamster embryos with water soluble vitamins: pantothenate stimulates blastocyst production. Hum Reprod 2000; 15:157-164.

163. Yi YC, Chen MJ, Ho JY, Guu HF, Ho ES. Mitochondria transfer can enhance the murine embryo development. J Assist Reprod Genet 2007; 24:445-449.

164. Takeda K, Tasai M, Iwamoto M, Onishi A, Tagami T, Nirasawa K, Hanada H, Pinkert CA. Microinjection of cytoplasm or mitochondria derived from somatic cells affects parthenogenetic development of murine oocytes. Biol Reprod 2005; 72:1397-1404.

165. Piko L, Matsumoto L. Number of mitochondria and some properties of mitochondrial DNA in the mouse egg. Dev Biol 1976; 49:1-10.

APPENDIX

TABLE 3 List of materials utilized

Name of materials	Source
35mm petri-dish	Nalge NUNC International, Rochester, NY, USA
60mm petri-dish	Becton Dickinson labware, Franklin Lake, NJ, USA
Accuspin™ tube	Sigma-Aldrich, St Louis, MO, USA
ATP bioluminescent somatic cell assay kit	Sigma-Aldrich, St Louis, MO, USA
Beem capsule	Electron Microscopy Sciences, Hatfield, PA, USA
Bovine Serum Albumin (BSA)	Sigma-Aldrich, St Louis, MO, USA
CaCl2 2H2O	Sigma-Aldrich, St Louis, MO, USA
Citrate Dextrose Solution USP (ACD) Formula A	Baxter Healthcare Corporation, IL, USA
Dulbecco's PBS	Sigma-Aldrich, St Louis, MO, USA
EMBed 812	Electron Microscopy Sciences, Hatfield, PA, USA
EthyleneDiamineTetraacetic Acid (EDTA) (disodium salt)	Sigma-Aldrich, St Louis, MO, USA
Female/male golden Syrian (HsdHan™ AURA) hamster	Harlan Laboratories, Indianapolis, IN, USA
G200-Cu grid	Electron Microscopy Sciences, Hatfield, PA, USA
Glutamine	Sigma-Aldrich, St Louis, MO, USA
Glutaraldehyde	Electron Microscopy Sciences, Hatfield, PA, USA
Heat-inactivated fetal bovine serum	Sigma-Aldrich, St Louis, MO, USA
Heparin	Abraxis, IL in USA
Hepes	Sigma-Aldrich, St Louis, MO, USA
Histopaque	Sigma-Aldrich, St Louis, MO, USA
holding pipette(9-17μm, 60mm, 30°)	SWE MED, Kungsbacka,Sweden
Human Chorionic Gonadotropin (hCG)	Sigma-Aldrich, St Louis, MO, USA
Hyaluronidase	Sigma-Aldrich, St Louis, MO, USA
JC-1 dye	Invitrogen, Eugene, OR, USA
KCl	Sigma-Aldrich, St Louis, MO, USA
KH_2PO_4	Sigma-Aldrich, St Louis, MO, USA
lead citrate	Electron Microscopy Sciences, Hatfield, PA, USA
LightCycler DNA FastStart SYBR Green kit	Roche, Mannheim, Germany
Medium 199	Invitrogen, Grand Island, NY, USA
MgSO4 7H2O	Sigma-Aldrich, St Louis, MO, USA
microinjection pipette(4μm, 60mm, 30°)	SWE MED, Kungsbacka,Sweden
Mineral oil (embryo tested)	Sigma-Aldrich, St Louis, MO, USA
Minimum Essential Eagle Medium	Sigma-Aldrich, St Louis, MO, USA

TABLE 3 Continued

Name of materials	Source
MitoTracker Green FM	Invitrogen, Eugene, OR, USA
MitoTracker Red CM-H_2XROS	Invitrogen, Eugene, OR, USA
Na Lactate (60% soln)	Sigma-Aldrich, St Louis, MO, USA
Na Pentobarbital (60mg/ml)	Sheris, Phoenix, AZ, USA
Na Pyruvate	Sigma-Aldrich, St Louis, MO, USA
NaCl	Sigma-Aldrich, St Louis, MO, USA
NaHCO3	Sigma-Aldrich, St Louis, MO, USA
Norm-Ject Syringe (5ml)	Henke Sass Wolf, Germany
Osmium Tetroxide	Electron Microscopy Sciences, Hatfield, PA, USA
penicillin-streptomycin	Sigma-Aldrich, St Louis, MO, USA
Plasmid isolation kit	Qiagen, Germany
Pregnant Mare's Serum Gonadotropin (PMSG)	Sigma-Aldrich, St Louis, MO, USA
Primer	Synthesized by Integrated DNA Technologies, Inc, Coralville, IA, USA
Propylene Oxide	Electron Microscopy Sciences, Hatfield, PA, USA
Square petri dish	Becton Dickinson labware, Franklin Lake, NJ, USA
somatic cell ATP releasing reagent	Sigma-Aldrich, St Louis, MO, USA
Sucrose	Sigma-Aldrich, St Louis, MO, USA
Surflo 16Gx2" I V catheter	Terumo Corporation, Japan
Taurine	Sigma-Aldrich, St Louis, MO, USA
TOPO-cloning vector	Invitrogen,Carlsbad, CA, USA
Tricine	Sigma-Aldrich, St Louis, MO, USA
uranyl acetate	Electron Microscopy Sciences, Hatfield, PA, USA

TABLE 4 List of instruments utilized

Name of Instrument	Type of Instrument
Thomas Ultra Air Pac-Air compressor	Thomas Ultra Air Pac-Air compressor
Cell disruption bomb	Parr Cell Disruption Bomb
LSM510Meta Confocal microscope	Zeiss, Oberkochen, Germany
Dissecting stereomicroscope	Ziess, Eastern Microscope Co , Raleigh, N C
Homogenizer	Dounce Homogenizer
LightCycler Probe Design Software 2 0	Roche, Indianapolis, IN, USA
Light Microscope	Nikon Diaphot
MetaMorph 7 5	Molecular Devices, Inc Sunnyvale, CA, USA
microtome	RMC-MT2C ultramicrotome for EM
microsurgical scissors	No ST-SAS-15, ASSI, Accurate Scientific & Surgical Instruments, Westbury, N Y
Needle (26-Gauge)	B-D, Becton Dickinson, Baxter Diagnostics Inc , Scientific Products Division, Columbia, MD, USA
pico-injector	PLI-100 pico-injector
plate luminometer	Dynex MLX microtiter plate luminometer
Real-time PCR	Roche LightCycler 480 system
SPSS 18 0	Chicago, IL, USA
Syringe (1ml)	B-D, Becton Dickinson, Baxter Diagnostics Inc , Scientific Products Division, Columbia, MD, USA
Transmission electron microscope	JEM-1200EXI electron microscope
Watchmaker forceps	ASSI, No ST-JFC-7

TABLE 5. List of components of medium.

Name of medium	Components	Concentration (mM)
M199TE [122]	Medium 199 (1X)	
	Taurine	5.0
	Hepes	25.0
	Heat-inactivated fetal bovine serum	1ml/20ml M199
	Penicillin-streptomycin	50IU/ml
Hamster Embryo Culture Medium-9 (HECM-9) [162]	Polyvinyl Alcohol (PVA)	0.1mg/ml
	NaCl	113.6
	KCl	3.0
	CaCl2	1.9
	MgCl2	0.5
	NaHCO3	15.0
	DL-Na-lactate	4.5
	1M HCl	1.4µl/ml
	Taurine	0.5
	Asparagine	0.01
	Cysteine	0.01
	Histidine	0.01
	Lysine	0.01
	Proline	0.01
	Serine	0.01
	Aspartic Acid	0.01
	Glycine	0.01
	Glutamic Acid	0.01
	Glutamine	0.2
	Ascorbic Acid	0.01
	Biotin	0.005
	Choline Cl	0.005
	Folic acid	0.003
	Inositol	0.003
	Niacinamide	0.005
	Pantothenate	0.003
	Pyridoxal	0.001
	Riboflavin	0.001
	Thiamine	0.003
M2 (for hamster sperm collection) [122]	NaCl	81.62
	KCl	4.8
	KH2PO4	1.18
	MgSO4	1.18
	CaCl2	1.7
	Na Lactate	31.3
	Na pyruvate	0.27
	EDTA	0.11
	Glutamine	1.0
	BSA	5 mg/ml
	Penicillin-streptomycin	100 IU/ml
ST 20 homogenization medium [156]	Sucrose	8.0% (w/v)
	Tricine-NaOH	20 mM
	EDTA	1 mM
	pH	7.4

TABLE 6 Abbreviations

Abbreviations	The full name
PGC	primordial germ cells
FSH	follicle stimulating hormone
LH	luteinizing hormone
IVF	*In Vitro* Fertilization
Yrs	years
Yo	Year-old
GnRH	Gonadotropin-releasing hormone
IP	Intraperitoneally
hCG	Human chorionic gonadotropin
ICSI	intracytoplasmic sperm injection
CDC	Center for Disease Control and Prevention
ATP	adenosine triphosphate
OMM	outer mitochondrial membrane
IMM	inner mitochondrial membrane
IMS	inter-membrane space
mtDNA	mitochondrial DNA
ROS	reactive oxygen species
ETC	electron transport chain
NADH	nicotinamide adenine dinucleotide
$FADH_2$	flavin adenine dinucleotide
OH	hydroxyl radical
H_2O_2	hydrogen peroxide
MMP	mitochondrial membrane potential
MPTP	mitochondrial membrane permeability transition pore
VDAC	voltage-dependent anion ion channel
ADP	adenosine diphosphate
rRNA	ribosomal RNA
tRNA	transfer RNA
M II	metaphase II
ANT	adenine nucleotide (nt) translocator
M I	metaphase I
SER	smooth endoplasmic reticulum
Δ4,977	deletion of mtDNA 4977bp
TEM	Transmission Electron Microscopy
IVC	inferior vena cava
IACUC	Institutional Animal Care and Use Committee
ODU	Old Dominion University
ANOVA	Analysis of Variance
PMSG	Pregnant Mare's Serum Gonadotropin

TABLE 6. Continued.

Abbreviations	The full name
hrs	hours
min	minutes
COC	Cumulus oophorus cells with oocyte complex
JC-1	5,5',6,6'-tetrachloro-1,1,3,3'-tetraethylbenzimdazoylcarbocyanine iodide
DMSO	dimethyl sulfoxide
MRR	MitoTracker Red CM-H_2XROS
MGF	MitoTracker Green FM
QPCR	Real-time polymerase chain reaction
GA	glutaraldehyde
PB	phosphate buffer
PBS	Phosphate buffered saline
BSA	bovine serum albumin
NMA	Methyl-5-Norbornene-2,3-Dicarboxylic Anhydride
DMP-30	Dimethylaminomethyl phenol
DDSA	dodecenyl succinic anhydride
CL	cytoplasmic lamellae
FDA	Food and Drug Administration
MEM	Eagle's minimum essential medium
IP	intraperitoneally
HECM-9	hamster embryo culture medium 9

VITA

Department of study
Department of Biological Sciences, Old Dominion University, Norfolk, VA 23529

Education
Ph.D Biomedical Sciences (2009-2011) Old Dominion University, Norfolk, VA
M.S. Biology (2005-2008) Old Dominion University, Norfolk, VA
M.S. Pathology and Pathophysiology (2000-2003) China Medical University, Shenyang, China
M.D Clinical Medicine (1995-2000) Dalian Medical University, Dalian, China

Professional Membership
ASRM- American Society of Reproductive Medicine
UMDF- United Mitochondrial Disease Foundation

Honors and Awards
1. The Virginia S. Bagley Endowed Scholarship, Fall 2009-Spring 2010, Old Dominion University.
2. Travel Award for academic meeting, 2010, Old Dominion University.

Scientific Presentations
1. The 66th Annual Meeting of American Society of Reproductive Medicine, Denver, CO, 2010
   Fang Li, Wentia Ford, Fatma S.Duran, Frank J. Castora, Howard W. Jones and R. James Swanson.
   "Mitochondrial changes in aged oocytes and improvement of fertility rate through autologous platelets mitochondrial microinjection" (Oral presentation)
2. Mitochondria Medicine Symposium, Phoenix, AZ 2010
   Fang Li, Wentia Ford, Fatma S.Duran, Frank J. Castora, Howard W. Jones and R. James Swanson. "Autologous mitochondria transfer from platelets to improve fertility rate." (Poster)
3. Society for the Study of Reproduction , Pittsburgh, PA July 18-22 2009
   Wentia Ford, Fang Li, Frank Castora, Howard Jones, and R James Swanson. "Age-related morphologic and microscopic variations in Syrian hamster ovaries and oocytes." (Poster)

Publications

1. Fang Li, Wentia Ford, Fatma S.Duran, Frank J. Castora, Howard W. Jones and R. James Swanson. Mitochondrial changes in aged oocytes and improvement of fertility rate through autologous platelets mitochondrial microinjection. Fertility and Sterility, 2010;94(4):S57
2. Song N, Jia XS, Jia LL, Ma XB, Li F, Wang EH, Li X. Expression and role of Oct3/4, Nanog and Sox2 in regeneration of rat tracheal epithelium. Cell Prolif 2010; 43:49-55.
3. Expression and role of Notch signalling in the regeneration of rat tracheal epithelium, Ma XB, Jia XS, Liu YL, Wang LL, Sun SL, Song N, Wang EH, Li F. *Cell Proliferation.* 2009; 42(1):15-28.
4. Kazuhisa Hasui, Fang Li, Xin-shan Jia et al. An immunohistochemical analysis of gastric B-cell lymphomas: Stromal cells exhibit peculiar histogenesis in gastric B-cell lymphomas. *Acta Histochem, Cytochem*, 2003; 36(2):153-164.
5. Kazuhisa Hasui, Fang Li, Xinshan Jia et al. Direct DNA sequence analysis of immunoglobulin heavy chain gene variable region in Chinese gastric lymphomas. The proceedings of the seventh Japnase-Korean Lymph reticular workshop.2002:74-80.
6. He'anguang, Jiaxinshan, Li Fang. Pathological analysis to 21 cases of early lung cancer. *The Second International Symposium of Molecular Pathology*, 2001:16.
7. Jiaxinshan, Kazuhisa Hasui, Li Fang et al. Study on 80 cases of EBER-1 ISH of malignant lymphoma. The Second International Symposium of Molecular Pathology, 2001:37.
8. Fang Li, Xinshan Jia. Actuality and expectation of tele-pathology. *Progress in Japanese Medicine*, 2001, 22(11):520.